SOIL
Discussions

Open Access

EGU

Meso- and microplastic distribution and spatial connections to heavy metal contaminations in highly cultivated and urbanised floodplain soilscapes – a case study from the Nidda River (Germany)

Collin J. Weber[1], Christian Opp[1], Julia A. Prume[2,3], Martin Koch[2], Peter Chifflard[1]

5 [1]Department of Geography, Philipps-University Marburg, 35032, Germany
[2]Department of Physics, Philipps-University Marburg, 35032, Germany
[3]Bayreuth Graduate School of Mathematical and Natural Sciences (BAYNAT), University of Bayreuth, 95447, Germany

Correspondence to: Collin J. Weber (collin.weber@geo.uni-marburg.de)

Abstract

10 Floodplain soilscapes act as temporary sinks in the environment and are nowadays affected by multiple contaminant accumulations and exposures, including heavy metals and (micro-)plastics. Despite increasing knowledge of the occurrence and behaviour of (micro-)plastics at the interface between aquatic and terrestrial systems, there are still major uncertainties about the spatial distribution of plastics, their sources and deposition, as well as spatial relationships with other contaminants. Our recent case study addresses these questions, using the example of a river system ranging from rural to urban areas. Based

15 on a geospatial sampling approach we obtained data about soil properties, heavy metal contents via ICP-MS analyses, and particle-based (171 µm – 52 mm) plastic contents, analysed using sodium chloride density separation, visual fluorescence identification and ATR-FTIR analysis. We found plastic contents of 0.00–35.82 p kg^{-1} and heavy metal enrichment (Enrichment factor 1.1–5.9). Levels of both contaminations occur in the lower range of known concentrations and show a different spatial distribution along the river course and in the floodplain cross-section. Furthermore, we found that plastic

20 enrichment occurs in the uppermost soil layers, while heavy metal enrichment is located at greater depths, indicating different sources and deposition periods. Finally, direct short to long-term anthropogenic impacts, like floodplain restoration or tillage may affect plastic enrichments, raising questions for future floodplain management.
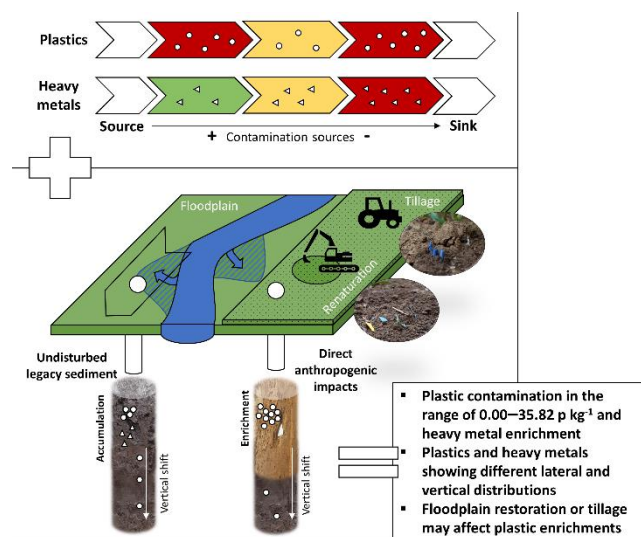
Keywords

25 *Plastic, Heavy metal pollution, Wetland, Soil, Fluvial, Density separation*

1 Introduction

After an initial half-decade of investigating plastic contamination in terrestrial environments, and with increasing progress in the development of suitable analytical methods, it has become clear that our soils contain far more plastics than perhaps previously assumed (Möller et al., 2020; Qi et al., 2020; Zhang et al., 2020; Braun et al., 2021). After plastics were detected

30 in soils of different soilscapes, from highly cultivated to semi-natural scapes (Huerta Lwanga et al., 2017; Zhang and Liu, 2018; Liu et al., 2018; Corradini et al., 2019; Piehl et al., 2018), whether microplastics can be found in soils, appears no longer to be the major question. Rather, the question now is about where, and to what extent, high concentrations of plastics can be found, what spatial differences exist and what the reasons are for different susceptibility levels of soils to plastics?

When talking about plastics in soilscapes, there are various definitions and size classifications resulting from the different

35 research disciplines dealing with plastic contaminations in the environment (Hartmann et al., 2019). Plastics in the environment can be defined as solid and insoluble, polymeric or co-polymeric, human-made particles that are produced (primary form) or fragmented by biogeochemical and physical processes (secondary form) to a certain size range (Bancone et al., 2020; Andrady, 2017). A widely applied size designation is microplastics (MP): in the past usually as defined as particles ranging from 1 μm to 5000 μm (Andrady, 2017), but currently defined according to ISO/TR 21960:2020 as particles with a size between 1 μm

40 and 1000 μm (International Organisation for Standardisation, 2020). Additionally, particle size-based distinctions can be made between nanoplastics (< 1 μm), large microplastics (1–5 mm), coarse microplastics (2–5 mm), meso- (> 5 mm) and macroplastics (> 25 mm) (Hartmann et al., 2019, Weber and Opp, 2020). Furthermore, plastics as environmental contaminants can be distinguished from other contaminants, like heavy metals, through their recent occurrence (exponential increase in

45 production of plastics since the 1950s) and the absence of geogenic background levels, due to the purely anthropogenic production of the materials (Zalasiewicz et al., 2016; Dong et al., 2020).

Potential impacts from plastics in general, but especially MP particles on soils, comprise influences on soil structure, material balance, the release of pollutants or the uptake of plastics into the food chain (Wang et al., 2019; Wang et al., 2020). For example, plastic particles can have a negative influence on soil aggregation and bulk density (Souza Machado et al., 2018), or have potentially adverse effects on the activity of microorganisms as well as soil animals, depending on concentration and

50 particle size (Rillig et al., 2017a; Selonen et al., 2020). Small MP especially can have a negative impact on plant growth or can be absorbed by plants, thus entering the food chain and ultimately the animal and human body (Rillig et al., 2017b; Rillig et al., 2019; Karbalaei et al., 2018; Ragusa et al., 2021). Furthermore, dissolution of additives from plastics (e.g., heavy metals and plasticisers) which are partly persistent and toxic, or an accumulation of pollutants on plastics, could be observed in marine and terrestrial environments (Catrouillet et al., 2021; Hahladakis et al., 2018). Studies from marine and aquatic environments,

55 as well as laboratory experiments, demonstrated that microplastics adsorb (e.g., Cu, Pb) or desorb (e.g., Cd, Zn) heavy metals (Munier and Bendell, 2018; Holmes et al., 2012). For soil environments the adsorption of heavy metals, depending on polymer type and particle shape, was detected (Verla et al., 2019). Finally, the presence of MP in soils can influence the heavy metal behaviour, like a reduction of the exchangeable, carbonate-bound and Fe-Mn-oxide bound fraction, while increasing the organic-bound fraction of the metals (Yu et al., 2021; Yu et al., 2020).

60 Floodplains and their soils today are primarily characterised by a "human-natural entanglement" (Edgeworth, 2011), resulting in deposited legacy sediments, and are in a conflict of use through the diverse natural services and anthropogenic beneficial activities (e.g., flood retention versus construction or agricultural land). Due to their spatial location in an aquatic-terrestrial interface, floodplain soils are exposed to unique influences, and have been subject to the constant impact of natural and anthropogenic pollutants (e.g., lead, copper, PAHs) (Dudka and Adriano, 1997; Price et al., 2011; Hürkamp et al., 2009). For

65 example, floodplain soils can act as an accumulation site for heavy metals, which are released in the catchment area in addition to geogenic contents by historical mining, industry or traffic (Ciszewski and Grygar, 2016; Lair et al., 2009; Opp et al., 1993). Floodplains cover only 0.5–1% of Earths land area, but river networks contain a significant portion of global plastic demand (Nardi et al., 2019; D'Elia et al., 2017). As the semi-terrestrial part of fluvial transport corridors in the global plastic cycle, and with a dominant transport direction from land to sea, floodplains could have an important role as temporary transfer and

70 deposition areas of plastics (Siegfried et al., 2017; Lechthaler et al., 2020; Kiss et al., 2021). Plastics can enter floodplain areas, and therefore floodplain soilscapes, through direct small-scale inputs (e.g., littering, sewage sludge application on fields) (Corradini et al., 2019; Piehl et al., 2018) or diffuse, more spacious inputs like surface runoff (from slopes) (Rehm et al., 2021) or flood water delivery (Christensen et al., 2020; Weber and Opp, 2020). Incorporated plastics can accumulate in the youngest and uppermost floodplain soil layers due to sedimentation since the 1960s, or agricultural utilisation, but also reaches deeper

75 soil layers through in-situ displacement (Weber and Opp, 2020; Cao et al., 2021). Spatial distribution of plastics in floodplain soils seems to have a clear drop with the soil depth (Cao et al., 2021; Weber et al., 2021; Weber and Opp, 2020), but a heterogenous lateral distribution. Christensen et al. (2020) found in some parts higher plastic loads in the floodplain than in

the stream channel, which may relate to remobilisation of deposited plastics, and exports during floods at the river channel (Hurley et al., 2018; He et al., 2021). The lateral distribution has been linked to population density in the catchment (Scheurer

80   and Bigalke, 2018, Christensen et al., 2020), land use (direct input agriculture) (Cao et al., 2021) and vegetation (trapping) (Weber and Opp, 2020) as well as floods (sediment deposition) (Weber and Opp, 2020; Lechthaler et al. 2021, Christensen et al., 2020) with some correlation between plastic content and soil texture (Christensen et al., 2020; Weber et al., 2021). Different levels of particle-based plastic concentrations have been documented in floodplain soils: In the Lahn River catchment (Hesse, Germany) Weber and Opp (2020) documented loads of 0.62–5.37 p kg^{-1} for mesoplastics (> 5 mm) and 0.31–8.59 p kg^{-1} for

85   coarse microplastics (2–5 mm), while Weber et al. (2021) report loads of 0.36–30.46 p kg^{-1} with a size of 219.0–8,321.0 µm (NaCl separation), where the mean size was 1171 µm and only a few particles occur with a size >2000 µm. A further study from Germany, investigating the Inde River (North Rhine Westphalia) documented average loads between 47.9 p kg^{-1} (depth profiles) and 25.4 p kg^{-1} (topsoils) for microplastics with a size between 500 and 5000 µm (canola oil extraction) (Lechthaler et al., 2021). Christensen et al. (2020) found 23–330 p kg^{-1} in proximal floodplain topsoils (0–4 cm) of three rivers in Virginia

90   (US) with average sizes of 290–1160 µm (NaCl separation), and Cao et al. (2021) report concentrations of 4.94–252.70 p kg^{-1} (5.0–0.1 mm, NaCl separation) down to 80 cm in intensively utilised agricultural soils of the lower Yangtze River floodplain (CHN).

Floodplain soils provide important ecosystem services: the retention of flood waters, their influence on the water balance, filtration and groundwater formation, and not least as a fertile site for food production, are worth mentioning. However, less

95   obvious functions such as the storage of soil organic carbon, estimated between 0.5–8.0 % of global soil organic carbon storage (D'Elia et al., 2017), or the retention of phosphorus (P) in deep P stocks, and the influence of riparian buffer zones on freshwater eutrophication, are further important functions (Weihrauch and Weber, 2020). In the meantime, it is becoming increasingly apparent that a wide variety of soil functions, and thus ecosystem services, are affected by plastic particles in soils (Selonen et al., 2020). Therefore, knowledge about the spatial distribution, the identification of hotspots in soilscapes, and the natural and

100   anthropogenic processes responsible for them, are indispensable for future risk assessments.

Furthermore, from a scientific perspective, the abundance of plastics in river sediments, both in and outside the stream channel, could also allow the study of recent sedimentary deposition processes based on plastic dating (Lechthaler et al., 2021; Turner et al., 2019). Plastic is discussed as a possible marker of the Anthropocene epoch (Zalasiewicz et al., 2016; Zalasiewicz et al., 2021; Waters et al., 2016), not least because of the material properties and worldwide occurrence. In addition to these more or

105   less strictly scientific considerations, the approach of plastic dating in sediments also offers the possibility to capture the temporal component of plastic pollution in river sediments and floodplain soils (Weber and Lechthaler, 2021). In view of possible prevention and management strategies of further plastic pollution in the environment, the temporal component, as well as the spatial component, should not be neglected.

Against the background of current research on MP in floodplain soils, and the still open questions on the origin, spatial

110   distribution, and interrelationships with other pollutants, this case study was conducted in a study area that is subject to a wide range of human impacts. The floodplains of the Nidda River and its catchment area can be considered very representative of

Central European River basins due to the clear sequence from the rural upper reaches over agricultural heartland to the highly urbanised lower reaches. Furthermore, the associated land use, possible point and diffuse plastic sources and the conflicts arising around the floodplain and watercourse management, are also comparable to many intensively utilised floodplain areas.

115 Due to the presence of various contaminants in floodplains, a consideration of plastics and a well-known contamination, here limited to heavy metals, can be purposeful, not least because of possible interactions.

Regarding the predominant catchment and soilscape properties, we aim to investigate the following aspects and related issues at the aquatic-terrestrial interface:

1. Occurrence of plastics in floodplain soils with regard to spatial and temporal contexts, proving the hypothesis that the
120 river course has a minor role in contrast to other factors (e.g., distance to the river), in spatial plastic distribution.

2. Relationships between plastics concentration and fluvial depositions, based on grain size and stratigraphy, proving the hypothesis that plastics enters floodplain soilscapes primarily through fluvial deposition.

3. Spatial relationships between heavy metals and plastics against the background of contamination patterns, investigating spatial correlations between both contaminants.

125 **2 Methods**

2.1 Study area

The Nidda River, with a length of 89 km, and its catchment with a total area of 1,942 km², are located in the Wetterau basin as part of the Hessian Depression in central Germany (Lang and Nolte, 1999). The Wetterau basin is flanked by the basaltic Vogelsberg mountains at the north-east, were the Nidda River rises at 720 metres above sea level (m. a. s. l.) and passes through
130 the basin in a south-westerly direction, guided by basalt ridges, until the river flows into the Main River at 85 m. a.s.l. (Figure 1). Except for the surrounding mountain ranges, namely the Vogelsberg (Tertiary basalt) and the Taunus (Rhenish slate mountains), the Wetterau basin consists of tertiary basalt ridges and marine and lacustrine sediments covered with up to 10– 15 m Pleistocene loess (Lang and Nolte, 1999; Kühn et al., 2017; Schmidt et al., 2010). In combination with a typical Central European climate (mean annual temperature 9 °C and precipitation of 650 mm), and very fertile soils due to the loess
135 accumulation, the Wetterau is an important cultural landscape, which has been inhabited and cultivated almost continuously since the early Neolithic period (Kühn et al., 2017; Jockenhövel, 1990). This long-lasting cultivation and deforestation also influence the soilscapes of the catchment area. While the upper reaches and upland positions are dominated by Cambisols developed in periglacial solifluction layers (basalt), the remaining catchment area is dominated by soils developed on loess (Luvisols, Regosols, relictic Chernozems, Stagnosols). In small valleys, depressions and lower slopes, colluvial deposits cover
140 the former land surfaces (Kühn et al., 2017).

The floodplains of the Nidda River first appear after leaving the Vogelsberg (headwaters) and progressively expand with the river course; they consist mainly of Fluvisols (fine-grained Holocene flood loam and colluvial deposits) and partly of Gleysols and Stagnosols (Table A 1). Floodplains, except for the direct riparian zones, are often cultivated as crop land, meadows and

pastures. Large parts of the floodplains are part of a landscape conservation area for the protection of wet meadows and near-

145 natural floodplain areas. However, the amount of land used for residential development and infrastructure facilities is also

increasing, reaching a high level in the Frankfurt metropolitan area, and restricts near-natural or just cultivated floodplain areas

severely.

The Nidda River itself, as a spatial connection through the basin landscape, can be classified as a medium-sized stream system

with six major tributaries (Figure 1). Located in the cultural landscape, the stream is influenced by intense industrial and

150 agricultural activities, including six industrial and municipal wastewater treatment plants in its course, and river engineering

for flood protection (Brettschneider et al., 2019; Schweizer et al., 2018) (Figure 1). Today's land use along the Nidda River

changes from a rather rural environment in the upper reaches (population density: 72 people km², settlement and traffic area:

10.6 %) to a heavily cultivated agricultural heartland in the middle reaches (population density: 282 people km², settlement

and traffic area: 16.1 %), to the highly urbanised lower reaches in the Frankfurt metropolitan region (population density: 3077

155 people km², settlement and traffic area: 58.6 %) (Hessian State Statistical Office, 2021).

Flood events under the hundred-year flood level (< HQ100) occur frequently between December and February in flood

retention areas along the river course, with a total area of 44.8 km² (Regional Council Darmstadt, 2015). Flood protection

measures, such as dams, widening of the cross-section, or flood retention basins in the catchment area, have been constructed

since the 1920s and have been continuously expanded (Regional Council Darmstadt, 2015). Nevertheless, ten high flood events

160 with a discharge > 25.7 m³ s⁻¹ for the gauge Nieder-Florstadt (ID: 24830050, between sampling sites OKA and FRA) occurred

between 1967 and 2011, showing an average discharge of 28.2 m³ s⁻¹ (max: 37.6 m³ s⁻¹ in 1981), average discharge rate of

53.4 l (s km²)⁻¹ and an average water level of 308 cm (max: 343 cm in 1981) (Regional Council Darmstadt, 2015). The average

discharge during flood events exceeds the long-term middle discharge (MQ) of 3.0 m³ s⁻¹ by 9.4 times.

Due to the natural environmental conditions, as well as the utilisation and anthropogenic influences, the Nidda River is part of

165 a very characteristic catchment system, and comparable to many medium-sized rivers in central Europe. Intensive agricultural

use, a high proportion of residential development and infrastructure, urban agglomeration in the lower reaches and diverse

wastewater discharges, result in multiple possible point and diffuse (micro-)plastic sources, increasing along the river course.

2.2 Soil sampling

The selection of sampling sites was carried out with the aim of implementing a geospatial approach and identifying sites

170 representative of the floodplain landscape and its different soilscapes as already introduced by Weihrauch (2019), as well as

Weber and Opp (2020). The selection was carried out with the help of a preliminary evaluation of geodata (aerial photos,

geological map, soil map, morphology) and the following conditions: each sampling site a) must be representative of a stretch

of watercourse with typical soil formations and landscape characteristics (Weihrauch, 2019), b) must be located in the

designated floodplain (10–100 year flood events), c) should not be located in close proximity to potential MP point sources

175 (e.g., garbage dump, sewage plant), and d) should be free of interruptions (infrastructure, dams) in the floodplain cross-section

(Weber and Opp, 2020). Furthermore, each site should consist of a clear structure of floodplain morphology including levee, inactive flood channels and back swamp (Weber and Opp, 2020)

In contrast to other catchments, the anthropogenic utilisation and land use in the Nidda catchment was the major restriction for the identification of suitable sampling sites. Except for the headwaters, where no floodplain can be found due to narrow valley morphology, there are still four areas in the middle and lower reaches of the Nidda that show a floodplain width of 400–900 meters (on one side) and have not been dammed excessively. In these areas, which are part of the protected landscape area "Floodplain Association Wetterau," four transect locations were selected after a preliminary soil survey, in order to represent the floodplain cross-section (Figure 1). Each transect location can be reached by annual floods, and would be flooded by 50–200 cm (sites NID and MOK) or 1–100 cm (sites OKA and FRA) during a hundred-year flood (Regional Council Darmstadt, 2015). Furthermore, the transect locations are partly affected by river and floodplain renaturation measures. Land use comparison based on satellite images from 1933 and 2020 show that arable land changed to grassland at the distal floodplain of site OKA, and floodplain renaturation is taking place at sites NID, MOK and FRA (Figures S2 and S3).

Finally, soil sampling was conducted during summer 2019 and 2020 at the river transect locations, using pile core driving with stainless-steel cores (diameters of 100 mm and 80 mm) down to a depth of 2 m. At each site, two (NID, FRA) or three (MOK, OKA) points were sampled, each localised in the proximal or distal floodplain area, with an additional third point in the central floodplain at sites MOK and OKA as the floodplains are wider there. Sampling points were numbered as 1 (distal), 2 (central) and 3 (proximal) at sites MOK and OKA, 1 (distal) and 2 (proximal) at site NID and 1 (proximal) and 2 (distal) at site FRA.

At each sampling point of the transect, two complete cores at a distance of 5 m from each other, were extracted, resulting in 20 cores (Table A 1). Soil stratigraphy and pedogenesis were documented according to the FAO Guidelines for soil description (FAO, 2006), and classified according to WRB 2015 (IUSS Working Group, 2015) and German soil classification (Ad-hoc AG Boden, 2005). Samples were collected from the two cores with stainless-steel spatulas and pooled in the field according to fixed depth levels (10 cm sections in 0–0.5 m, 25 cm sections in 0.5–1.5 m and 50 cm section from 1.5–2.0 m), resulting in 10 composite samples per sampling point (total: 100 samples, 385.5–3,704.6 g dry fine earth per sample), and stored in corn starch bioplastic bags (Mater-Bi bags, BioFutura B.V., Rotterdam, Netherlands).

Additionally, plastics fragments on topsoil surfaces were sampled if a conspicuous amount of plastics could be found around the drill points (Piehl et al., 2018). Visible plastics fragments were collected on a 20 m² area around the drill points by walking straight lines with two persons (four-eyes-principle), according to Piehl et al. (2018). This additional procedure was conducted at the OKA sampling site (points OKA-2 and OKA-3).
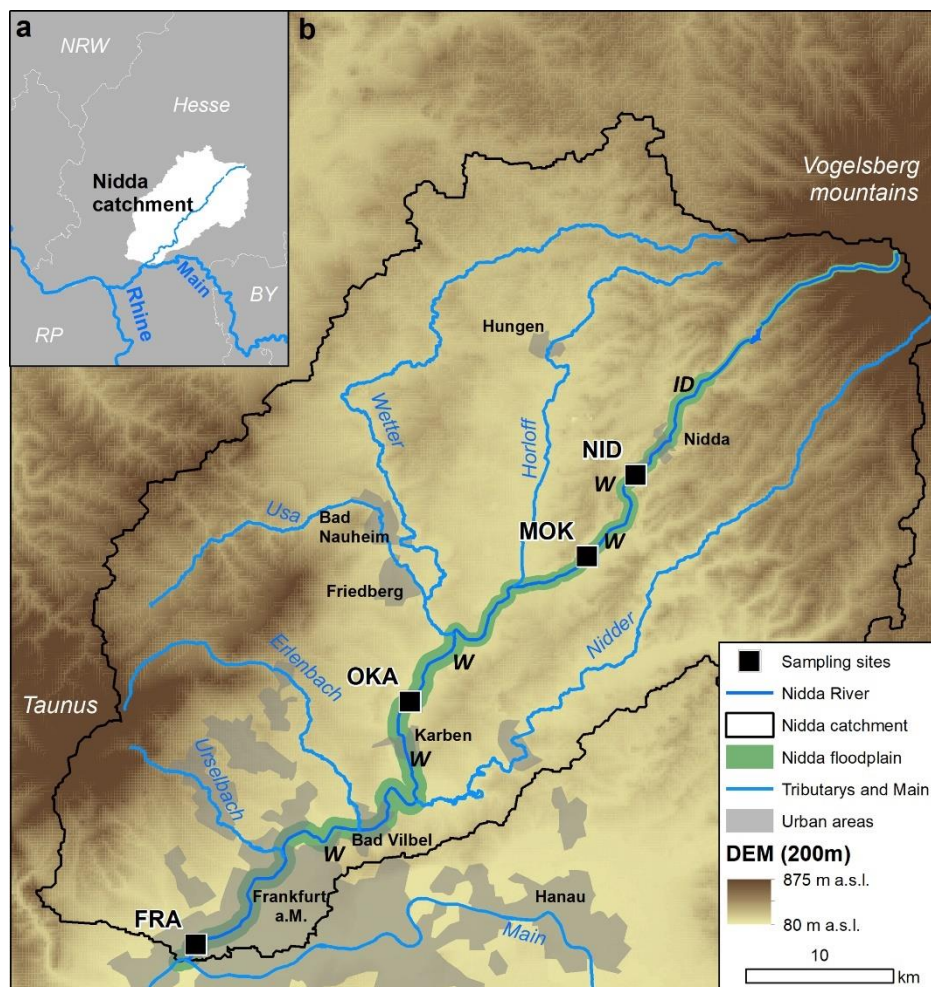
Figure 1: a: General map showing the location of the Nidda catchment in Germany. b: Nidda catchment with tributaries, transect locations and urban areas with location of wastewater treatment plants (W) and industrial dischargers (ID) along the Nidda river. Data source: NUTS 2021 (© EuroGeographics for the administrative boundaries), WISE Large rivers (© European Environmental Agency), Digital terrain model 1 (© Hessian Administration for Soil Management and Geoinformation) and urban areas (© OpenStreetMap contributors 2021. Distributed under the Open Data Commons Open Database License (ODbL) v1.0.). Detailed maps of transect sites and elevation profiles can be found in Figure S1.

2.3 Laboratory analysis

Field fresh soil samples were immediately dried at 45 °C for four days in a drying chamber. Subsequently the sample material was carefully mortared (ceramic mortar) to break down soil macro-aggregates, and dry-sieved through stainless-steel sieves (Retsch, Haan, Germany), covered with a stainless-steel plate, to the size fractions >5 mm (mesoplastics), >2 mm (coarse microplastics and rock fragments) and <2 mm (large microplastics and fine-earth fraction). The fine-earth fraction was afterwards homogenised in a stainless-steel bowl and divided via a rotary sampler (Retsch, Haan, Germany), to obtain representative sub-samples for soil parameter and metal analysis. Each fraction was stored in corn starch bags.

SOIL
Discussions

2.3.1 Soil parameter and metal analysis

220   The moisture content of representative sub-samples (<2 mm, average mass: 99.6 g) was determined by drying (105 °C), and the content of organic matter (OM) was determined via loss of ignition at 550 °C (DIN 19684–3:2000–08) and both were recorded as percentage by weight (wt%). Additionally, the pH was measured with a pH 91 electrode (WTW, Weilheim, Germany) in a 0.01 M $CaCl_2$ solution (m:V 1:2.5). Carbonate content was determined after reaction with a few drops of 3.23 M hydrochloric acid (HCl) according to Ad-hoc AG Boden (2005) and soil texture was analysed via the Integral Suspension

225   Pressure Method (Durner et al., 2017) after the samples had been prepared according to DIN ISO 11277:2002–08. Soil textures were reported according to Guidelines for soil description (FAO, 2006) and individual shares of clay, silt and sand, in percentage by weight (wt%).

Pseudo-total concentrations of the metal Fe, the metalloid As and the heavy metals V, Cr, Co, Ni, Cu, Zn, Cd, Hg, Pb were determined from digests of 1 g prepared subsample with 20 ml aqua regia (12.1 M HCl and 14.4 M HNO_3; ratio 1:3; DIN ISO

230   11466:2006-12). Metal concentrations were quantified using inductively coupled plasma–mass spectrometry (ICP–MS; XSERIES 2; Thermo Fisher Scientific, Bremen, Germany) and system calibration with a certified multi-element standard solution (ROTI®STAR; Carl Roth GmbH, Karlsruhe, Germany). Each digest was measured three times and averaged, resulting in converted results given in mg kg^{-1}. Relative standard deviation (RSD) after threefold measurements, and detection limits resulting from the multiplication of the mean standard deviation of 10 repeated blank measurements by factor 3, were used as

235   control (Voica et al., 2012; Thomas, 2001).

2.3.2 Plastics and microplastics analysis

Plastics and microplastics analyses were carried out according to the method and application first published by Weber & Opp (2020) and Weber et al. (2021). Visual identification with naked eye, or the help of a magnifying glass, and partly under a stereomicroscope (SMZ 161 TL, Motic, Hong Kong), was conducted for a) macro- and mesoplastics particles collected from

240   soil surfaces and b) mesoplastics and coarse microplastics particles manually selected from soil sample material (>2 mm) after dry-sieving. Potential plastic particles were cleaned (deionised water) (Jung et al., 2018), dried (45 °C), photographed and stored in rim jars for polymer identification.

The total fine-earth fraction (<2 mm) with a sample mass between 94.0 and 3552.1 g (mean: 1295.3 g) and a related average volume of 1053 ml (250–2750 ml), was used to separate out microplastic particles (Figure S4). For this purpose, a density

245   separation with the "MicroPlastic Sediment Separator" (MPSS) (Hydro-Bios Apparatebau GmbH, Kiel-Altenholz, Germany) under the application of a saturated and >300 µm filtered NaCl-solution (density adjusted to 1.2 g/cm³ and controlled by balance and aerometer) was performed. Density control, before and after separation, shows a range between 1.195 to 1.218 g cm³ with an average of 1.203 g cm³, at an average solution temperature of 19.47 °C (Figure S4). The sample solution was

SOIL
Discussions

Open Access
EGU

stirred for 60 minutes and then allowed to settle for 19 hours. At the end of the separation time, the integrated ball valve was

250 closed, and separated material was rinsed into glass beakers using filtered NaCl solution.

Afterwards, the remaining sample material, consisting of organic material and potential plastic particles, was separated into the following size classes using stainless-steel sieves (Ø 75 mm, Atechnik, Leinburg, Germany), and filtered (>50 µm) deionised water: >1,000 µm, >500 µm and >300 µm. After sieving, the sieve residues were filtered via vacuum-filtration on cellulose filters (Ø47 mm, LLG-Labware, Meckenheim, Germany), and then transferred to glass petri dishes (Ø90 mm or 200

255 mm) by rinsing with deionised water and drying at 50°C for two days, according to Prume et al. (2021).

To differentiate between organic material and potential plastic particles, a Nile Red staining procedure (20 µg mL^{-1} Nile Red ethanol-acetone (1:1) solution, Sigma-Adlrich, Taufkirchen, Germany) was applied (Maes et al., 2017; Konde et al., 2020). Nile red solution was applied with the help of a pipette and sprayer and stained for 10 minutes at 50 °C in a drying chamber (Konde et al., 2020). Stained petri dishes were afterwards visually inspected systematically under a stereomicroscope (SMZ

260 161 TL, Motic, Hong Kong), with fluorescence setup (Excitation: 465 nm LED; Emissions 530 nm colour long pass filter: Thorlabs, Bergkirchen, Germany) and transmitted light (Prume et al., 2021). This approach allows the visual identification of plastic particles, but is disrupted by the fluorescence of natural organic components in the red fluorescence range (e.g., chitin shell ants, freshwater mussel fragments), so the exclusion of organic particles must be based on surface structure (e.g., cell structures) or, in case of uncertainty, by spectroscopic analysis. Each fluorescent, or other potential plastic particle, that shows

265 no cellular or biologic structure and a clear and homogenic colour (Noren, 2012), was collected and individually stored in microplates (Brand, Wertheim, Germany). Each particle collected was then classified according to surface characteristics (particle type, shape, surface degradation, colour), photographed (Moticam 2, Motic, Hong Kong) and size measured (longest diagonal, Motic Images Plus 3.0, Motic, Hong Kong) (Hidalgo-Ruz et al., 2012; Noren, 2012).

Polymer type identification for a) previously visually determined mesoplastic to coarse microplasti particles, and b)

270 microplastic particles identified via staining-fluorescence procedure, was performed using the Tensor 37 FTIR spectrometer (Bruker Optics, Ettlingen, Germany) combined with a Platinum-ATR-unit (Bruker Optics, Ettlingen, Germany). Measurement was carried out using 20 background scans followed by 20 sample scans for each sample, with a resolution of 4 cm^{-1} in a wavenumber range from 4,000 cm^{-1} to 400 cm^{-1} (Jung et al., 2018; Primpke et al., 2017; Primpke et al., 2018). The ATR-unit used is the limiting factor for the lower size limit of the particles determined in this study, since particles with a size <300 µm

275 have insufficient contact area and are difficult to handle (Weber et al., 2021).

2.3.3 Contamination prevention

To prevent contamination of the samples with additional plastic particles, the use of plastic equipment in the field and laboratory was avoided. All devices used were made of glass, ceramic or stainless steel. All equipment was thoroughly rinsed with filtered water (>50 µm) after each use, and only filtered NaCl solution (>300 µm) and deionised water (>50 µm) was

280 used. Corn starch bags were used for sample storage and transport, and their spectrum (ATR-FTIR) was compared with all

identification spectra for safety reasons. Furthermore, the sample material was kept under cover whenever possible and cotton lab coats were used to avoid air contamination by fibres.

During microplastic separation and subsequent analysis steps, control for possible sample contamination was done by means of five blank samples randomly applied during the separation runs. In four of the five blanks, five fragments with an average

285   size of 294.9 µm ± 79.15 µm (SD) (B1: 3 fragments, B2: 1 fragment, B3: 1 fragment) and one filament (B4, length: 449.4 µm) were found via the staining-fluorescence procedure (examples given in Figure S5). The particles found in blank samples were too small or too degraded for polymer identification by ATR-FTIR. Blank control resulted therefore in an error of 1.2 particles per separation run or sample, but in a particle size below the determination limit of 300 µm, except one single fragment and filament. The calculated concentrations were therefore not adjusted.

290   **2.3.4 Statistics and data evaluation**

Data processing, basic statistical operations and data visualisation operations were conducted using Microsoft Excel (version 1808, Microsoft, Redmond, USA) or RStudio (version 1.3.1093, RStudio, PBC, 2020) within an R environment (version 4.0.3, R Core Team, 2020). Data processing of FTIR spectra was performed in OPUS 7.0 including atmospheric compensation and baseline correction (concave rubber band method) (Bruker Optics, Ettlingen, Germany) and in Spectragryph (Version

295   1.2.14; Menges, 2020; Oberstdorf, Germany). Spectra identification of pre-processed spectra was done via the OpenSpecy database using full spectra, and Pearson's r with $r^2 > 0.6$ as match quality indicator (Cowger et al., 2020). Spatial data was processed in ArcGIS (ArcMap version 10.8, Esri 2019, West Redlands, CA, United States).

In order to allow an effective assessment of spatial contamination differences between plastics and heavy metals, we calculated the heavy metal "Pollution load index" (PLI) based on "single pollution index" (PI) according to Kowalska et al. (2018)

300   following Eq. (1) and Eq. (2):

$$PI = \frac{HM}{GB} \tag{1}$$

$$PLI = \sqrt[n]{PI_1 \, x \, PI_2 \, x \, PI_3 \, x \, PI_n} \tag{2}$$

where HM is the concentration (mg kg^{-1}) of individual heavy metals (V, Cr, Co, Ni, Cu, Zn, Cd, Hg, Pb) and the metalloid As, and GB is the geochemical background concentration, calculated for the individual metals (V: 38.25 mg kg^{-1}, Cr: 25.0 mg kg^{-1}

305   ^{1}, Co: 8.75 mg kg^{-1}, Ni: 24.0 mg kg^{-1}, Cu: 13.25 mg kg^{-1}, Zn: 58.5 mg kg^{-1}, Cd: 0.14 mg kg^{-1}, Hg: 0.04 mg kg^{-1}, Pb: 27.0 mg kg^{-1}, As: 8.0 mg kg^{-1}) based on the average values from 341 soil samples (64 floodplain silt substrates, 277 floodplain sand substrates from Hessian floodplain soils (Friedrich and Lügger, 2011). In addition, the "Enrichment factor" (EF) was calculated in order to measure the potential impact of anthropogenic metal pollution against geogenic background contents (Kowalska et al., 2018) following Eq. (3):

310   $$EF = \frac{\left[\frac{HM}{LV}\right] sample}{\left[\frac{HM}{LV}\right] GB} \tag{3}$$

where HM is the concentration of individual heavy metal and LV the reference content of Fe concentration (mg kg^{-1}). Index values were also evaluated according to Kowalska et al. (2018) for PLI levels around 1 as "only baseline levels of pollution" and >1 with "deterioration of soil quality", and for EF with "deficiency to minimal enrichment" at values <2 and "moderate enrichment" at values between 2–5.

315   Plastic loads were documented as particles per kg soil dry weight (p kg^{-1}), including the total number of sufficient ATR-FTIR identified particles per sample (sample mass 94.0 to 3552.1 g). From 263 particles, previously identified visually (>2 mm, coarse soil fraction) or via staining-fluorescence procedure, 35 particles (13.31 % of all collected particles) were identified as organic (non-polymeric) with an R^2 between 0.77 and 0.96 for the spectra correlation by the OpenSpecy database. These organic particles were excluded from the entire data evaluation, which means that 228 particles are counted and evaluated as

320   sufficiently (R² > 0.6) identified as plastics. Ages of possible earliest occurrence (EPO age) were assigned to the particles identified based on the year of polymer development or start of production, according to Weber and Lechthaler (2021). Macro- and mesoplastic loads on soil surfaces from sampling at site OKA were reported as particles per square meter (p m²).

All data collected do not display a normal distribution (Shapiro-Wilk test) and, in some cases, show significant differences in variance by group. Comparison of means was carried out using the Wilcoxon test or Kruskal-Wallis test, using R standard

325   functions. Data visualisation was conducted with R standard functions (R Core Team, 2020), "ggplot2" (Wickham, 2016: https://ggplot2.tidyverse.org) and "corrplot" (Wei and Simko, 2017: https://github.com/taiyun/corrplot). Spearman correlation was performed with a significance level of p ≤ 0.05, and correlation coefficients were interpreted as: weak (r_{SP} 0.4 – <0.6), clear (r_{SP} 0.6 – <0.8), and strong (r_{SP} >0.8). Plotting and evaluation of three-dimensional data was carried out using the package "plot3D" (Soetaert, 2019: https://CRAN.R-project.org/package=plot3D) and additional multiple linear regression model.

330   **3. Results**

3.1 Plastic loads and features

In the floodplain soils along the Nidda River, plastic particles were found at each transect site and sampling point, resulting in a positive rate of 73 % of all samples (n = 100) which contain plastics. In each sample 0 to 20 particles (average: 2.64 particles, SD: 3.49) were found; overall concentrations range from 0 p kg^{-1} up to a maximum of 35.82 p kg^{-1}, with an average of 3.23 p

335   kg^{-1} (± 1.75 p kg^{-1} RSD, n = 100). Samples containing no detectable plastic particles occur mainly at depths > 75 cm, whereas higher concentrations can be found in the upper 30 cm of each soil column (Table 1).

340

SOIL
Discussions

Open Access

EGU

Table 1: Plastic concentration (p kg⁻¹) in soil samples (for plastics size range 171 μm – 52 mm).

Sampling depth (cm)	Plastic concentration (p kg^{-1})									
	Transect NID		Transect MOK			Transect OKA			Transect FRA	
	1	2	1	2	3	1	2	3	2	1
0–10	2.92	15.14	11.78	0.00	1.10	4.77	35.82	11.44	7.76	5.80
10–20	4.58	3.61	13.86	0.00	0.00	2.48	19.39	4.93	1.40	4.45
20–30	27.25	4.18	1.26	0.00	2.61	5.16	2.76	2.07	3.98	5.43
30–40	2.22	0.71	3.47	2.27	1.94	2.18	2.57	1.81	2.20	21.27
40–50	0.00	12.00	2.32	1.65	1.87	0.00	1.49	1.92	5.83	0.00
50–75	0.55	0.43	0.14	1.04	1.34	0.44	0.00	0.00	1.71	2.36
75–100	1.01	1.57	2.27	0.00	0.00	0.48	0.77	0.00	2.04	1.40
100–125	0.00	0.00	0.00	5.60	5.18	0.00	1.66	0.00	2.09	0.63
125–150	0.70	0.00	5.11	0.00	3.76	1.80	0.00	0.00	1.45	0.59
150–200	0.00	1.59	1.67	0.00	0.00	0.00	0.00	0.00	0.00	0.00

345

The extracted and identified plastic particles appear as films (45.8 %) and fragments (38.3 %), or as filaments, pellets and foams (Figure 2b), with weathered (49.0 %), fresh (28 %) or incipient alteration (23.0 %) surface structures. The shape composition consists of irregular (71.0 %), regular (25.0 %) or rounded (4.0 %) shapes; particle colour is often transparent or white (49.0 %), or bright red (16.0 %), blue (9.0 %) or pink (8.0 %), followed by different colours with an individual share ≤
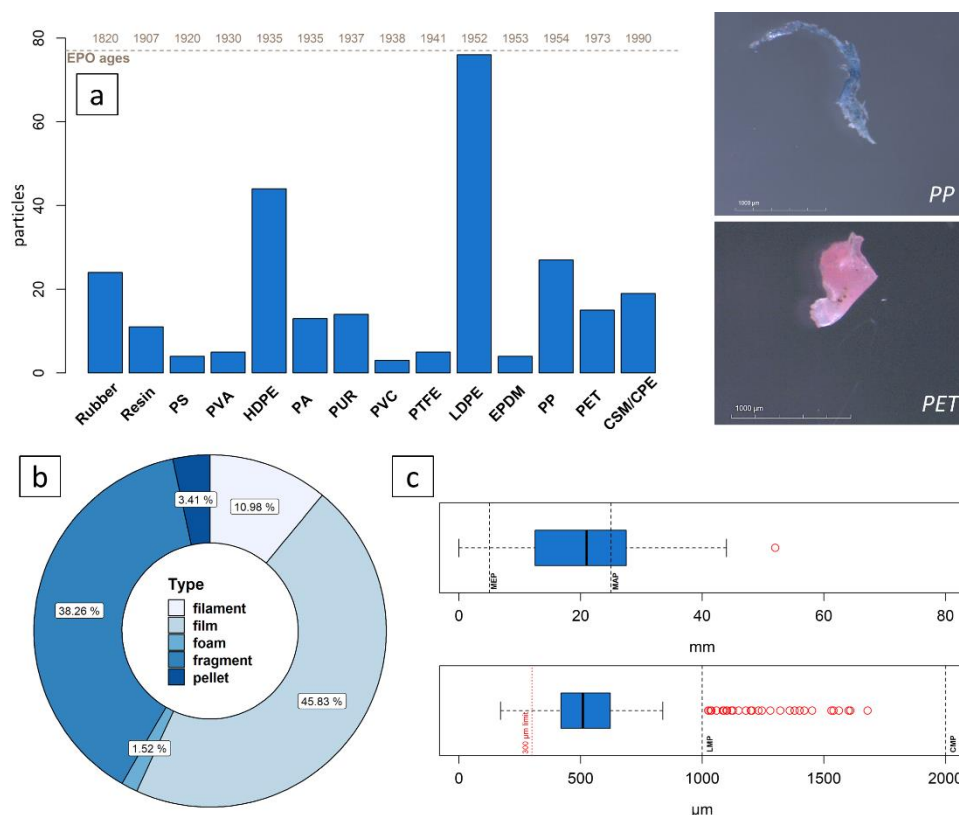
350   6.0 % (e.g., black, orange, yellow).

Figure 2: Particle feature composition. a: Number of identified polymer types (n = 228) sorted by age of earliest possible occurrence (EPO ages) with example of a blue PP film and pink PET fragment (Polymer type abbreviations explained in Table S2); b: Particle type composition (n = 228); c: Particle size composition for particles in coarse soil fraction (upper boxplot, n = 35) and fine soil fraction (lower boxplot, n = 193).

Polymer type composition is dominated by low- and high-density polyethylene (LDPE and HDPE) making up 46.0 %, followed by polypropylene (PP, 10.0 %), rubbers (9.0 %), chlorinated or chlorosulfonated polyethylene (CPE, CSM, 7.0 %) and polyethylene terephthalate (PET, 6.0 %) (Figure 2a). All identified polymers show a density of ≤ 1.2 g cm³ in pure form, except PET with 1.37 g cm³ (Cutroneo et al., 2021), which was thus only recorded semi-quantitative based on the density separation method with NaCl.

Plastic particles in the coarse soil fraction (>2 mm) occur in a size range between 2.1 mm and 52.0 mm, with an average of 20.68 mm (Figure 2c), while in the fine soil fraction (<2 mm) particle size ranges between 171.0 μm and 1680 μm with an average of 598.6 μm and a clear accumulation of outliers over 1000 μm (Figure 2c).

Additionally, sampling of plastics on the soil surface (site OKA), shows an occurrence of 1 p m² (OKA-3) to 1.05 p m² (OKA-2). The macroplastics collected occur as films (54.8 %), fragments (38.7 %) or styrofoam (6.5 %), with mainly irregular and weathered surfaces and an average size of 66.3 mm (Table S1). The plastics contain of HDPE (35.5 %), LDPE (16.1 %), PP (12.9 %) and other polymers like PET, polyvinyl chloride (PVC), polystyrene (PS) or polymethyl methacrylate (PMMA). In

14

some cases, the function of plastic items is still identifiable, for example, DIY store shield, fries fork, bottle cap or food wraps (Figure S6).

3.2 Heavy metal concentrations and soil properties

All of the 9 heavy metals analysed, as well as the metalloid As and the metal Fe, were detectable by ICP-MS measurement with contents above the detection limit. In relation to the mean values (n = 100), the content decreases from Fe (21,026.3 mg kg⁻¹) > Zn (55.4 mg kg⁻¹) > Ni (31.17 mg kg⁻¹) > Cr (29.82 mg kg⁻¹) > Pb (23.78 mg kg⁻¹) > Cu (16.58 mg kg⁻¹) > V (16.30 mg kg⁻¹) > Co (10.93 mg kg⁻¹) > As (6.63 mg kg⁻¹) > Cd (0.28 mg kg⁻¹) to Hg (0.11 mg kg⁻¹). A comparison with geogenic background and legislation values is possible for the heavy metals Cr, Ni, Cu, Zn, Cd, Hg and Pb. All of those heavy metals show higher average concentrations in deeper soil (50–200 cm) than in upper soil (0–50 cm) layers (Table 2). Mean and median values fall below the worldwide average contents of surface horizons (Kabata-Pendias, 2011), but exceed the geogenic background values for Hessian floodplain soils in the case of Cr, Ni, Cu, Cd and Hg. Legislative precautionary values are exceeded by all heavy metals except Hg by the respective maxima (Table 2); these levels occur in individual samples at sites FRA-1, MOK-1 to MOK-3, NID-2 and OKA-3 at varying depths between 20 and 200 cm.

Table 2: Summary of heavy metal contents compared to geogenic background levels and legislation values with calculated pollution indices and their thresholds.

		Elemental concentrations								Indices	
		Cr	Ni	Cu	Zn	Cd	Hg	Pb		PLIᵃ	EFᵇ
		mg kg⁻¹								(-)	(-)
Mean		29.8	31.2	16.6	55.4	0.28	0.11	23.8		1.1	2.2
Median		26.3	27.6	13.5	40.0	0.16	0.07	17.7		0.9	1.8
Min.		9.8	8.7	3.5	17.0	0.05	0.01	8.3		0.4	1.1
Max.		75.4	100.7	55.8	194.5	1.39	0.46	77.1		3.2	5.9
Mean upper soil	0–50 cm	28.6	29.9	15.1	50.1	0.25	0.09	22.9		1.0	2.1
Mean lower soil	50–200 cm	31.1	32.5	18.1	60.8	0.31	0.13	24.6		1.2	2.4
SHWᶜ	Average content surface horizons worldwide	60.0	29.0	38.9		0.41		27.0	lowᶠ	<1	<2
GBHFᵈ	Geochemical background in Hessian floodplain soils (0–2 m)	25.0	24.0	13.3	58.5	0.14	0.04	27.0	moderateᶠ	1	2–5
PVᵉ	Precautionary values	60.0	50.0	40.0	150.0	1.00	0.50	70.0	highᶠ	>1	>5

ᵃ Pollution load index; ᵇ Enrichment factor; ᶜ Kabata-Pendias (2011); ᵈ Friedrich & Lügger (2011); ᵉ German Federal Soil Protection Ordinance - BBodSchV (1998); ᶠ Pollution assessment according to Kowalska et al. (2018) with low pollution or enrichment, moderate/baseline pollution or enrichment and high/significant pollution or enrichment

With regard to the calculated pollution indices, the Pollution load index (PLI) ranges between 0.4 and 3.2, with a mean of 1.1,
385   just above the limit value of 1 at which baseline levels of pollution begin. The PLI of maximum concentration values of 3.2
indicates a partial deterioration of soil quality (Kowalska et al., 2018). The values of the Enrichment factor (EF) are also
comparable, with a mean just above the limit where a moderate enrichment can be assumed, and maximum values indicating
a significant pollution enrichment. Moderate enrichment and pollution occur at all sites, irrespective of depth. However, higher
PLI and EF average values are also found in deeper soil layers (50–200 cm) (Table 2), and significant pollution enrichment
390   based on EF > 4 occur at all locations except FRA, at depths below 100 cm.

Soil conditions for heavy metal behaviour in the floodplain soils investigated consist of predominantly silty to clayey soils
(soil textures: SiCL, SiC, C), OM contents range from 1.57 wt% up to 24.91 wt% with an average of 8.33 wt% and pH values
indicate a very weak acidic environment with a total average of 6.33 (range 4.90–7.69, moderate acid to weak alkaline) (Table
A 2). Furthermore, in groundwater affected Fluvisols or Gleysols, pedogenic oxides (Fe, Mn) in Bl-horizons as well as
395   reductive conditions occur (Table A 1).

Deviations in soil texture occur only in subsoils (>100 cm), where the sand content increases locally, and at the middle and
lower reaches, with average values up to 22.0 wt% (OKA-1) or 30.5 wt% (FRA-2). Similarly, organic enrichment occurs
through deep peat bands or layers with OM contents of 16.2 wt% (NID-2, >125 cm) or 24.9 wt% (MOK-1, >100 cm).

3.3 Spatial distribution

400   ### 3.3.1 Plastics along the river course

Plastic concentrations along the river course show average site loads of 3.92 p kg^{-1} at site NID (upper middle reaches), 2.34 p
kg^{-1} at site MOK (middle reaches), 3.46 p kg^{-1} at site OKA (upper lower reaches) and finally 3.52 p kg^{-1} at site FRA (lower
reaches). Even though average plastic concentrations vary by ± 1.58 p kg^{-1} along the course, no significant (p = 0.5106)
difference exists between the mean values per sampling site. The same applies to the comparison of proximal mean values and
405   distal mean values along the course of the river. For example, the proximal sites show the following mean values in downstream
direction: 4.18 p kg^{-1} (NID), 1.78 p kg^{-1} (MOK), 2.22 p kg^{-1} (OKA) and 4.19 p kg^{-1} (FRA), without significant mean differences
(p = 0.6916); while distal sites reflect the following: 3.92 p kg^{-1} (NID), 4.18 p kg^{-1} (MOK), 1.73 p kg^{-1} (OKA) and 2.84 p kg^{-1}
(FRA). Regarding the plastic sums per sampling site (Figure 3), the highest sums for proximal sites are found in the upper
middle reaches (39.24 p kg^{-1}) and lower reaches (41.92 p kg^{-1}) (Figure 3a), while distal sites also show high values in upper
410   middle reaches, but differ in the middle reaches (41.87 p kg^{-1}) (Figure 3b). The highest average plastic content occurs in the
upper middle and the lower reaches, whereas the higher plastic amounts depend on the position in the floodplain cross-section.
Furthermore, sampling points impacted by direct anthropogenic influences (e.g., renaturation, earthworks) show the highest
plastic sums (Figure 3). A statistical correlation with the soil textures was not found (p > 0.63 for each texture fraction),
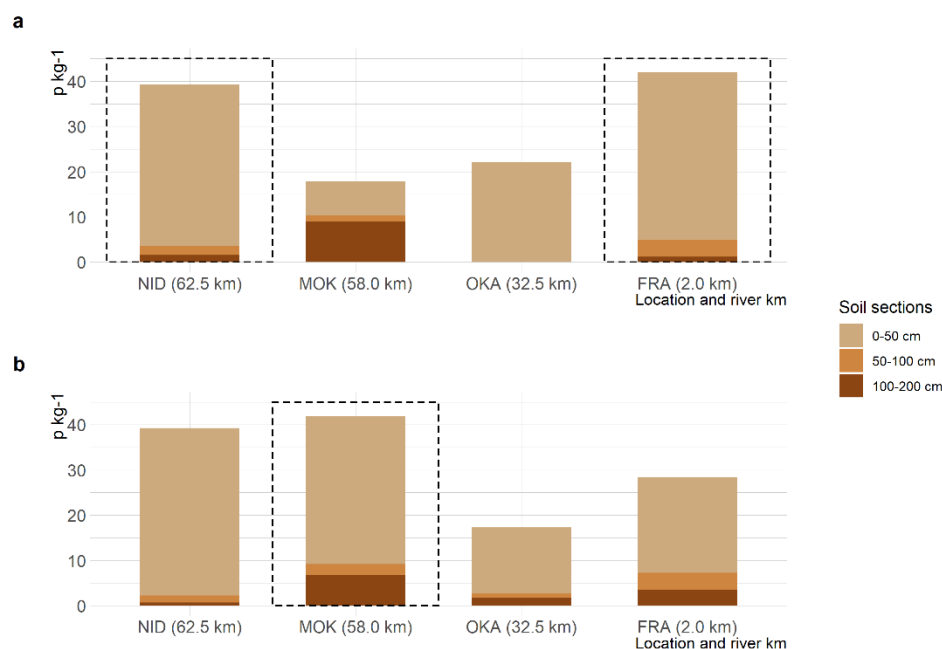although the sand content increases from the upper to the lower course while the clay content decreases (Table A 2).

Figure 3: Cumulative sum of plastic concentrations (p kg⁻¹) per sampling point divided in soil layers (0–50 cm, 50–100 cm, 100–200 cm) along the river course (with transect site location and river km). a: Proximal sampling points (21.4–35.5 m from active channel); b: Distal sampling points (203.4–859.7 m from active channel); dotted boxes indicate anthropogenic influence (renaturation, past earthworks).

3.3.2 Lateral and vertical plastic distribution in floodplain cross-transects

As mentioned before, there are no significant differences in average plastic loads at the lateral level in the floodplain cross-section (Figure 4). Average concentrations range from 4.12 p kg⁻¹ (n = 4) at proximal sites, over 6.82 p kg⁻¹ (n = 2) at central to 3.97 p kg⁻¹ (n = 4) at distal sites, while absolute maxima (35.82 p kg⁻¹ or 27.25 p kg⁻¹) occur at central and distal sites (Figure 4c). Increased plastic loads in central floodplain positions are dominated by accumulation of plastics in the arable topsoil of the OKA-2 site (Table A 1, Table A 2). A lateral sorting of the plastic sizes, depending on the distance to the channel, could not be determined (Figure S8). Meso- and single macroplastic particles only occur in the topsoils (plough horizons) of sites OKA-2 (central) and OKA-3 (proximal).
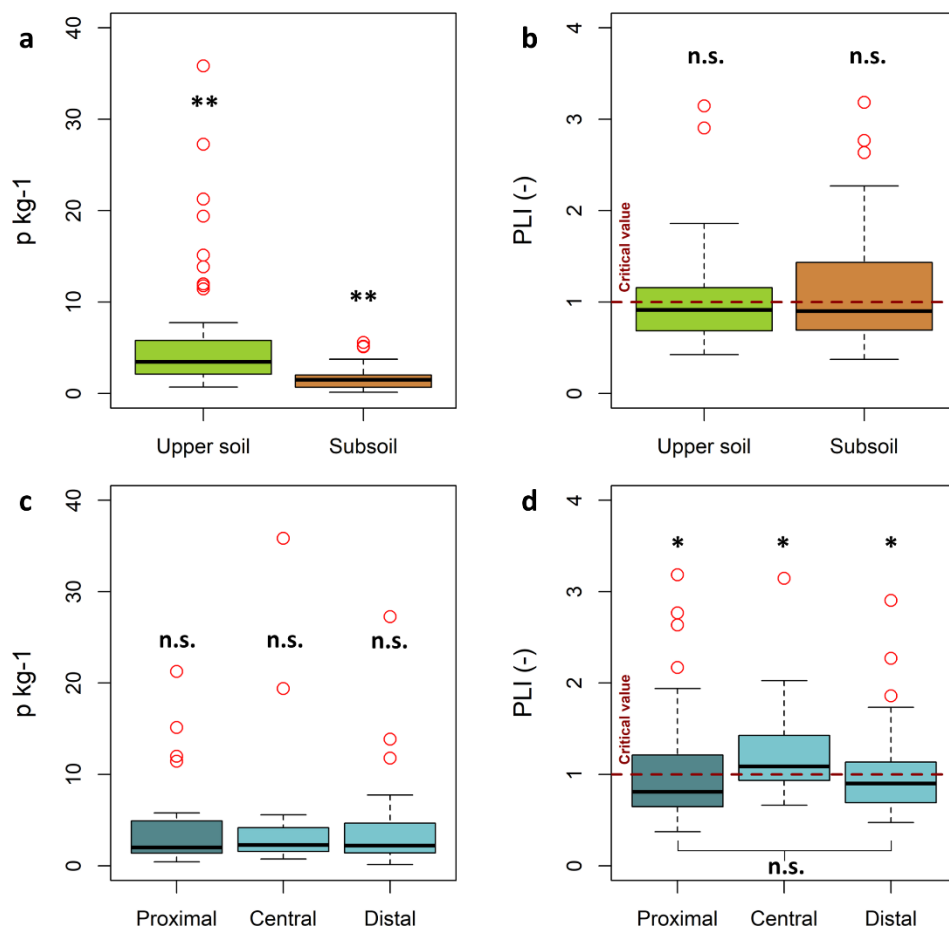
17

Figure 4: Plastic concentrations (p kg-1) and Pollution load index values by depth or floodplain position. a: Plastic concentrations without zero values (empty samples) for upper soil layer (0–50 cm, n = 43) and subsoil layer (50–200 cm, n = 30); b: Pollution load index for upper soil layer (0–50 cm, n = 50) and subsoil layer (50–200 cm, n = 50) with critical value (red dashed line) for significant pollution; c: Plastic concentrations without blank samples for proximal (n = 30), central (n = 11) and distal (n = 32) sampling points; d: Pollution load index for proximal (n = 40), central (n = 20) and distal (n = 40) sampling points with critical value (red dashed line) for significant pollution. Significance levels: p <0.01 (**); p <0.05 (*); p >0.05 (n.s.).

In contrast, clearly significant differences occur in the vertical plastic load distribution (Figure 4a). While the upper soil layers (0–50 cm), consisting of topsoil A-horizons as well as upper B-horizons, show an average plastic load of 6.36 p kg^{-1}, the subsoil layers consisting of B-horizons (50–200 cm) have a significantly lower mean value of 1.73 p kg^{-1} (p < 0.0000). The vertical distribution of plastic loads shows a clear maximum in the uppermost sampling layer (0–10 cm), mostly consistent with A-horizon boundaries, with an average of 9.65 p kg^{-1} continuously decreasing to a depth of 40–50 cm, with an average of 2.71 p kg^{-1} and even lower average values ranging between 1.52 p kg^{-1} and 0.33 p kg^{-1} below that (Figure 5). This vertical decrease is comparable to the decrease in mean organic matter content (with the exception of deeper >100 cm layers which contain peat), and the increase in mean sand content from a depth of 50 cm (Figure 5). Conspicuous accumulation in the

vertical distribution occur at sampling site NID-1 (27.25 p kg^{-1} at 20–30 cm), MOK-1 (11.78 p kg^{-1} to 13.86 p kg^{-1} at 0–20 cm), OKA-2 (35.82 p kg^{-1} to 19.39 p kg^{-1} at 0–20 cm) and FRA-1 (21.27 p kg^{-1} at 30–40 cm) (Figure S9).
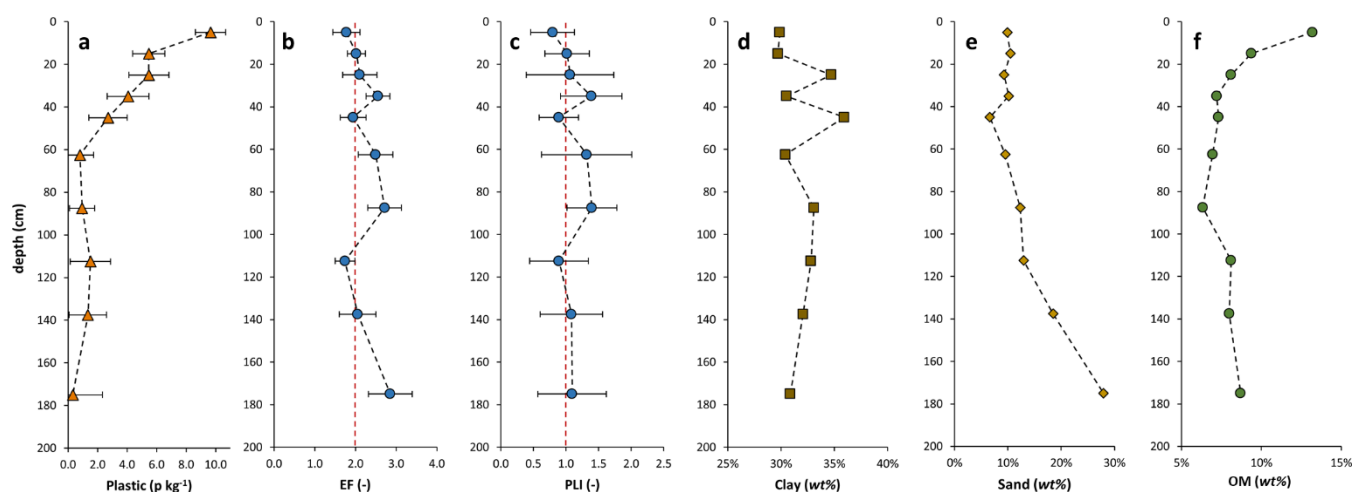
445

Figure 5: Depth distribution of average plastic concentrations, pollution indices and soil properties. a: Plastic concentration (n = 73); b: Enrichment factor (EF, n = 100) with critical value for significant enrichment (red dashed line); c: Pollution load index (PLI, n = 100) with critical value for significant pollution (red dashed line); d: Clay content (n = 100) in mass-% (wt%); e: Sand content 450 (n = 100) in mass-% (wt%), f: Organic matter content (OM, n = 100) in mass-% (wt%).

With regard to the vertical distribution of plastic particle characteristics, differences could be found between upper and deeper soil layers. Figure 6a indicates that particles with a size >2000 μm (coarse microplastic border) consist mainly of fragments and films, whereas smaller particles show a heterogenous distribution related to particle type, particle size and soil depth. Deepest soil layers are reached only by fragments and filaments: the share of particle types shows higher values of films (46.43 455 %) and fragments (41.04 %) in lower soil layers than in upper layers (films: 45.40 %, fragments 34.48 %). Overall, the particle size ranged from 171 μm to 52,000 μm (average: 4,566.49 μm) in upper soil layers (0–50 cm), and smaller average sizes of 512.15 μm (242–2,700 μm) in lower (50–200 cm) layers. The share of particle surface characteristics shows an increase for weathered particles with depth, from 45.98 % to 62.50 %, at the cost of fresh and incipient alteration particles.
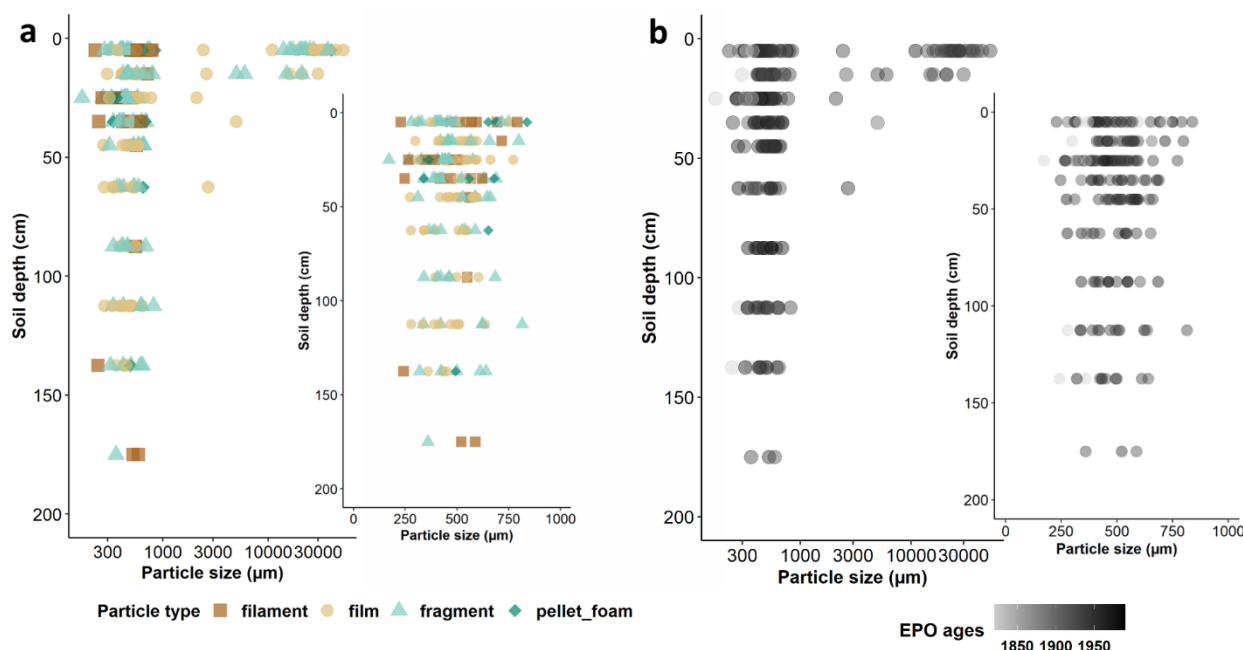
Figure 6: Depth distribution of plastic particle sizes classified according to (a) particle type and (b) age of possible earliest occurrence (EPO ages) for whole particle size range and focused on particles between 0–1000 μm (n = 228).

EPO ages ranging in upper and lower layers from 1820 to 1990, with an average occurrence of 1938 in upper (0–50 cm), and 1941 in lower (50–200 cm) layers, indicating no significant polymer age differentiation. The vertical distribution of EPO ages (Figure 6b) shows no clustering of polymers of the same age at certain soil depths. There is no dominant polymer type in the deep soil layers, and only two young (>1990) chlorosulfonated or chlorinated polyethylene (CSM/CPE) polymers occur. In general, the depth distribution of the youngest CSM/CPE polymer group shows an average depth of 23.5 cm and an enrichment in soil layers between 0 and 35 cm (third quartile of CSM/CPE depths, n = 24).

With regard to the identified division of plastic content, with values in upper soil layers higher than in deep layers, a statistical correlation with soil textures could not be proven. While in upper soil layers clays (C), silty clays (SiC) and silty clay loams (SiCL) prevail, deeper soil layers show primarily silt loams (SiL), loams (L) or sandy loams (SL), and loamy sands (LS) (Figure S10). Comparing the mean plastic contents of both soil texture groups, with 3.26 p kg^{-1} for more clayey (n = 56) and 3.32 p kg^{-1} for rather loamy-sandy (n = 44) samples, no significant (p = 0.3845) difference appears.

3.3.3 Spatial relationships to heavy metal contamination

As stated earlier, and contrary to the distribution of plastic occurrence, higher PLI and EF values are found in deeper soil layers, with significant pollution enrichments below 100 cm. Figure 7 illustrates the differences between plastic occurrence and PLI loads, showing a clear accumulation of plastics in upper soil layers (0–50 cm), with individual increased concentrations in deeper soil layers. In contrast, the PLI values show enrichment in soil layers between 40 and 120 cm, with EF concentrations showing an additional enrichment in deep soil layers below 150 cm (Figure 5b).
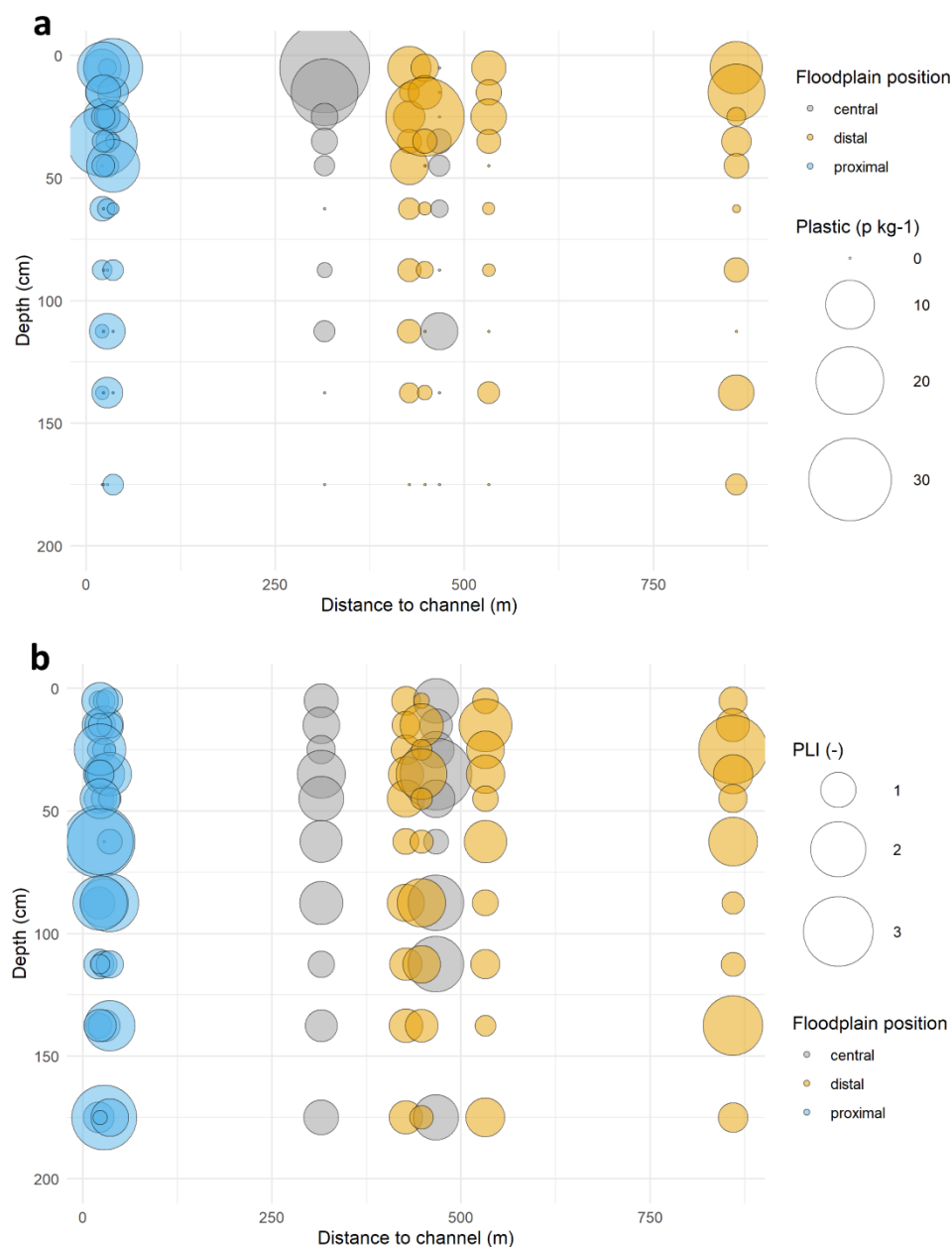
Figure 7: Lateral and vertical distribution of plastic concentrations and Pollution load index levels (point size as a function of plastic content or PLI levels). a: Plastic concentration (n = 100); b: PLI levels (n = 100).

With regard to the lateral distribution of heavy metal enrichment on the catchment scale, average EF values per site increase slightly from NID (upper middle reaches) at 2.06, MOK (middle reaches) at 2.42 and OKA (upper lower reaches) at 2.44, and then decrease to 1.97 at site FRA (lower reaches). The PLI values rank around 1, with a PLI <1 at sites FRA or MOK, and PLI >1 at sites OKA or NID (Table A 2). The lateral distribution on the floodplain cross sections shows slight differences, with an

21

increase from proximal (average PLI: 1.04, average EF: 2.11) to central (average PLI: 1.32, average EF: 2.41), and a decrease from central to distal (average PLI: 1.03, average EF: 2.26) sites.

A concise assessment of the spatial distribution differences is possible using multiple linear regression models, displayed as regression surfaces in Figure 8a and Figure 8b. Both regression surfaces show different orientations (slopes) and differences

490 among the variables in terms of their influence on each other. For the first comparison of plastic loads (Figure 8a) a significant influence ($p = 0.0111$) from the predictor variable, soil depth (cm), with regression beta coefficients of -3.0974 (t-value, $p = 0.0028$) and an estimated average effect -0.4094 could be observed. Therefore, changing soil depth is significantly associated with changes in plastic loads, but the distance to channel shows no significant association. For the second comparison with Enrichment factor (EF) values (Figure 8b), no significant associations were found between EF and the two predictor variables

495 ($p = 0.2066$). Those findings are also visible in the regression surfaces and illustrate the different data distributions. Whereas the plastic load regression surface (Figure 8a), with an intercept of 7.20, shows a clear slope along the soil depth axis (slope: -0.0493) and a hardly recognisable slope along the distance axis (slope: 0.0002), the EF regression surface (Figure 8b), with an intercept of 1.87, shows very little slope along the depth (slope: 0.0030) and distance (0.0005) axes. Therefore, it can be inferred that the enrichment of heavy metals shows a homogeneous spatial distribution, both to soil depth and across the

500 floodplain width, whereas the distribution of plastic content is found to be heterogeneous and significantly influenced by depth: decreasing with increasing depth.
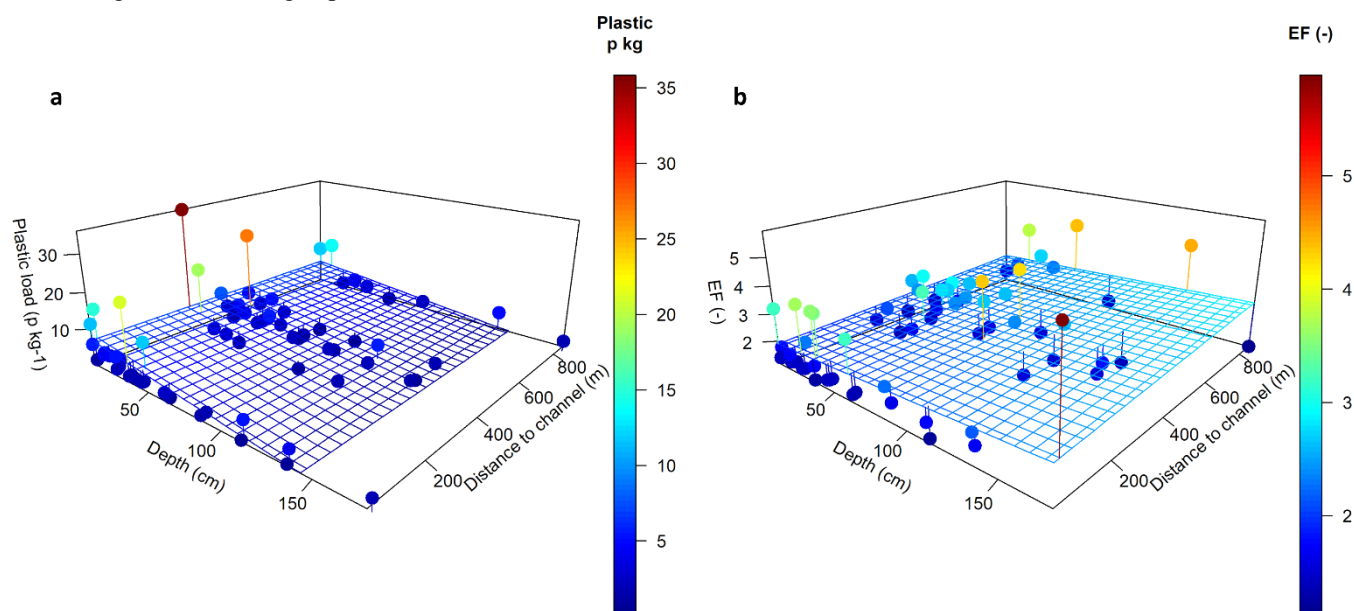

Figure 8: Three-dimensional visualisation of plastic loads and Enrichment factor (EF) levels in dependence of soil depth (cm) and distance to channel (m). Colour scale represents plastic loads or EF level. Regression surface (grid) based on multiple linear
505 **regression model for the three included variables. a: Plastic load (n = 100); b: Enrichment factor (n = 100).**

This spatial connection, and the influence of soil depth on plastic loads, is supported by a significantly ($p < 0.05$) weak negative correlation (r_{SP} = -0.56). Furthermore, plastic loads show slight negative correlations with EF (r_{SP} = -0.19) and PLI values (r_{SP} = -0.12). Slight to weak positive correlations (r_{SP} 0.2–0.6) occur between the river course (km) and distance to channel (m)

510   with clay and OM content, as well as slight negative correlations with sand content. Notable correlations between clay or OM and heavy metals, indicating a strong absorbance to clay minerals or humic substances, could not be found. Inter-element correlations show clear to high positive correlations (r_{SP} 0.6–1.0), except for lower correlation coefficients (r_{SP} <0.4) for Cd, Hg, Pb with V, Cr, Fe, Co, Ni and partly As (Figure S11).

4. Discussion

515   ### 4.1 Plastic abundance

Plastics were found at all transect locations along the Nidda River. The observed plastic content, ranging from 0 p kg^{-1} up to a maximum of 35.82 p kg^{-1}, is in the lower range of previously determined plastic contents in floodplain soils. For example, Christensen et al. (2020) found plastic loads of 23.0–330.0 p kg^{-1} for average particle sizes of 280–1,160 μm (NaCl solution) in three river floodplains in Virginia (US), whereas Lechthaler et al. (2021) document average loads of 25.4–47.9 p kg^{-1} for

520   plastics with a size of 500–5,000 μm (canola oil separation) in the Inde River floodplain (Germany). Both studies investigated near-channel depositions (bank profiles, levee situations), with a focus on topsoils and single depth profiles. Further investigations, based on the same geospatial sampling approach as in the present study, and conducted in the more rural river system of the Lahn River (Hesse, Germany), found loads of 0.62–5.37 p kg^{-1} for mesoplastics (> 5 mm) and 0.31–8.59 p kg^{-1} for large microplastics (2–5 mm) based on sieving (Weber and Opp, 2020), as well as 0.36–30.46 p kg^{-1} for microplastics

525   sized 219.0–8,321.0 μm based on NaCl separation of the fine soil fraction (< 2 mm) (Weber et al., 2021). The average value of all samples from the Nidda catchment at 3.23 p kg^{-1} is comparable to the average values of 2.06 p kg^{-1} (mesoplastics), 1.88 p kg^{-1} (coarse microplastics) or 2.75 p kg^{-1} for microplastics from the Lahn catchment (Weber et al., 2021; Weber and Opp, 2020).

With regard to intensive agriculturally utilised floodplain soils of the lower Yangtze River floodplain, and the lower particle

530   size range investigated, the average of 37.32 p kg^{-1} (100–500 μm) in 0–80 cm soil depth, clearly exceeds the Nidda catchment average (Cao et al., 2021). In comparison to further studies which examine plastic contents in agricultural soils, it becomes clear that these clearly exceed the values from the Nidda floodplain (Liu et al., 2018; Zhang and Liu, 2018; Corradini et al., 2019; Piehl et al., 2018). This could indicate the role of intensive agriculture in the contribution of plastic inputs. In the Nidda catchment, plastic enrichment through agriculture is also probable. The maximum plastic load (35.83 p kg^{-1}) and higher values,

535   especially for meso- and macroplastic contents, occur where plastic accumulation is also visible at the surface (site OKA, agricultural field). Plastic particles collected on soil surfaces at site OKA (Figure S6; Table T1) could be partially identified as parts of consumer articles. The identification of consumer articles may also indicate local littering as a potential source. At

this sampling site, the occurrence of plastics on soil surfaces at 1.0–1.05 p m² is clearly above the value of 0.021 p m² (206 p ha^{-1}) reported by Piehl et al. (2020) for microplastic particles on an agricultural farmland in Germany. Nevertheless, the

540 comparability of the studies is limited, especially because different separation solutions are used, and different particle sizes are considered. Higher plastic contents in agricultural soils could therefore also be caused by the consideration of particles < 300 µm in other studies.

With a view to the entire aquatic-terrestrial interface, it seems that floodplain soils contain lower plastic loads than river sediments in the active channel (riverbed, shore). For example, shore sediments of the Main River contain plastic loads of

545 786.0–1,368.0 p kg^{-1} (63–5,000 µm) and values > 50 p kg^{-1} for particles > 200 µm directly before and after the inflow of the Nidda River (Klein et al., 2015). Even in more rural areas, such as the Tisza River (eastern central Europe) contents reach values of 3,808 ± 1,605 p kg^{-1} (90–5,000 µm, zinc chloride solution) already in the upper reaches (Kiss et al., 2021). Both examples exceed the plastic concentration in the Nidda River floodplain by a multiple factor which, however, may be traceable in part to the examination of smaller particles in the comparative studies. Up to now, only the results of Christensen et al.

550 (2020) suggest equal or slightly increased levels in floodplain samples instead of channel samples, while larger plastic particles occur in floodplain deposits.

Plastic particle characteristics found in floodplain soils of the Nidda River are comparable to other findings from floodplain soils, as well as river sediments. Films and fragments prevail, followed by filaments and pellets, with a typical distribution for soils, with the exception that filaments are sometimes dominant in other studies (Christensen et al., 2020; Corradini et al.,

555 2019). Most of the particles show a weathered or incipient alteration surface structure, indicating prolonged exposure to degradation factors (e.g., physical break, UV-light) (Hidalgo-Ruz et al., 2012; Napper and Thompson, 2019; Chamas et al., 2020). The increase in the number of particles with smaller particle size also shows a typical distribution independent of the environmental media studied (Kooi and Koelmans, 2019). Due to the method used, particles <300 µm could only be detected semi-quantitatively here if their size and degradation state allowed a manual ATR-FTIR measurement. Therefore, it can be

560 assumed that plastic concentrations would still increase significantly at a lower detection limit, as in studies quantifying particles <300 µm (Cao et al., 2021).

The dominant polymer types found correspond to those of commonly produced and used polymers in Europe (top 10 ranking), like polyethylene (PE), polypropylene (PP), polyethylene terephthalate (PET) or rubbers (PlasticsEurope, 2018, 2020). This polymer composition, resulting from the frequency of use in everyday life, industry, agriculture and infrastructure (e.g., rubber

565 car tires), is also found in most soil studies, with fluctuations around the most dominant polymer type (Cao et al., 2021; Christensen et al., 2020; Lechthaler et al., 2021). Furthermore, a composition following the frequency of use is also found in channel bed sediments and seems to overlap in different river systems (Kiss et al., 2021; Hurley et al., 2018). For river shore sediments of the Main River, Klein et al. (2015) found a composition of PE, PP, PVC and dominant polystyrene (PS) which occupies only a small share <6 % in Nidda floodplain samples. Based on the density separation fluid used here, polymers with

570 a density >1.2 g cm³ can only be detected semi-quantitatively (e.g., PET). However, except for PET, and without taking

SOIL
Discussions
Open Access
EGU

additives into account, the common polymer types show a density <1.2 g cm³. Considering the binding of plastic particles to and in soil aggregates, the question arises whether all particles could be separated (Rehm et al., 2021; Zhang and Liu, 2018)? Although manual mortaring allows a gentle sample preparation, it does not dissolve soil microaggregates in which plastic might still be retained (Möller et al., 2020).

575 Besides the methodological limitations described, the comparison of plastic contents with other investigations, results frequently in restrictions based on methodical differences. These differences arise from different sampling concepts, the sample quantity examined, size classes, and the different separation methods. It is therefore difficult to evaluate the plastic content against the background of a contamination assessment, as is usual for other pollutants. In the previous discussion, mainly studies on floodplain soils (mostly near bank and topsoil), which work by means of density separation (NaCl or canola oil),

580 were consulted. Against the background of the comparisons made, it can be cautiously assumed that the contamination level of plastics over the entire soil depth of 2 meters is in the lower range of known contamination, also with regard to smaller particles. Thus, the Nidda floodplain and its soils could be classified as less contaminated against river sediments of larger rivers (e.g., Rhine, Main) and soils under intensive agricultural usage. However, the composition of the plastic particles in terms of shapes, size and polymers shows a typical composition for soils or fluvial sediments in general.

585 **4.2 Heavy metal abundance**

Heavy metals and the metalloid As are present in the floodplain soils of the Nidda River catchment. Even if the average concentrations of Cr, Ni, Cu, Zn, Cd, Hg and Pb fall below the average contents of surface (topsoil) horizons worldwide (Kabata-Pendias, 2011), the exceeding of local geochemical background values of Cr, Ni, Cd and Hg indicates a contamination enrichment of those heavy metals compared to other regional floodplains in Hesse (Germany) (Table) (Friedrich and Lügger,

590 2011). From a legal perspective, only individual breaches of the precautionary values require legal measures (e.g., further investigations, risk designation), traceable to the absolute maximum values and therefore single enriched samples (Bundesregierung, 1998). A pronounced contamination from a single element could not be detected.

Pollution indices, like the Enrichment factor (EF), or Pollution load index (PLI), enable an assessment of the possible anthropogenic impact on heavy metal concentrations (Kowalska et al., 2018). Both indices show average values just above the

595 threshold values for moderate enrichment (EF; >2) and baseline pollution (PLI; >1), with a significant enrichment for single samples with EF >5. As both indices require a geochemical background value for calculation, the exceeding of the thresholds indicates a deviation of heavy metal loads from the theoretical natural background variation (Kowalska et al., 2018; Alloway, 2013). Elemental concentrations and pollution indices show higher mean values and maxima in lower soil layers (>50 cm) than in upper soil layers (0–50 cm) (Table 1). This pattern could indicate older contamination in deeper floodplain sediments,

600 or mobilised heavy metals that reach deeper soil horizons through relocation processes (Alloway, 2013; Hürkamp et al., 2009; Dudka and Adriano, 1997). However, against the background of possible heavy metal displacements, the soil properties indicate adsorption tendencies. Dominant silty to clayey, organic rich Fluvisols and Gleysols, provide good adsorption potentials on clay minerals, humic-substances and the formation of metal-humus-complexes (Alloway, 2013; Blume et al.,

2016). Furthermore, adsorbent pedogenic-oxides, and reductive conditions in groundwater effected layers, with single peat
605   layers in deeper soil sections, can increase the retention of heavy metals (Blume et al., 2016; Alloway, 2013; Calmano et al., 1993). Additionally, the very weak acid environment falls below the pH values for incipient mobilisation of Cd, Zn, Ni, but not for Cu, As, Cr, Pb and Hg, even in the minima (Blume et al., 2016; Calmano et al., 1993).

Due to spatially widespread moderate enrichment, and baseline pollution by heavy metals under strong adsorption tendencies, anthropogenic impacts on heavy metal enrichment can be assumed. Because of the vertical differences observed, this vertical
610   pattern could also be due to an historical heavy metal enrichment in deeper soil layers (higher mean contents and maxima), and a more recent one in upper soil layers. Possible older sources of heavy metal enrichment may include mining in the headwaters of the Nidda River (Vogelsberg mountains: iron ore and basalt mining), as well as early industrial metal processing throughout the river catchment (Hürkamp et al., 2009; Dudka and Adriano, 1997). Mining and metal industry represent one of the main sources of historical heavy metal enrichment in river floodplains before, and especially during the Industrial
615   Revolution from the 1850s onwards (Kern et al., 2021). In contrast, recent sources could be related to wastewater treatment plants, industrial and traffic discharges as point sources, or uptake of polluted legacy sediments, as well as erosion on agricultural land (Alloway, 2013; Martin, 2015; Pejman et al., 2015; Hahn et al., 2016). Former studies, assessing the ecological quality and ecotoxicological effects from channel sediments along the Nidda River, concluded that, other than the headwaters, the whole Nidda river is affected by anthropogenic chemical pollution (e.g., PAH, PCB, metals) (Schweizer et al.,
620   2018; Brettschneider et al., 2019). A relationship between anthropogenic point sources and ecotoxicological effects could not be proved, which leads to the assumption of diffuse sources for chemicals and consequently also for heavy metals.

4.3 Spatial differences between plastic and heavy metal contamination

The spatial pattern of plastic and heavy metal contamination observed, differs along the lateral as well as vertical spatial
625   extension. First, no enrichment of plastic concentrations along the river course could be found, whereas heavy metal enrichment increases slightly with the course of the river (Figure 3, Table A 2). Second, no significant differences in plastic concentrations occur in the floodplain cross-section, whereas heavy metal enrichment increases slightly from proximal to central, and decreases to distal floodplain soils (Figure 4). Therefore, the hypothesis that plastics accumulate with the river course cannot be supported, as also found for the Lahn river catchment by Weber et al. (2021).
630   Although plastic concentrations in floodplain soils could be related to the population densities in the river catchments (Scheurer and Bigalke, 2018; Christensen et al., 2020), and microplastic loads in river water show higher abundance near urbanised areas (Xiong et al., 2018), these patterns do not appear to be applicable on the Nidda River. Highest plastic occurrence was found at the proximal floodplain sites in the upper middle reaches (NID) and lower reaches (FRA). For riverbed sediments, Kiss et al. (2021) found plastic enrichment in tributaries of the Tisza River, indicating the contribution of plastic in suburban areas.
635   Although the Nidda rises in a rural landscape, passes through agricultural heartland and reaches the highly urbanised agglomeration area around Frankfurt, a simple source-to-sink downstream increase does not occur. Although, suburban to

rural areas also seem to provide potential plastic sources. In contrast, heavy metal abundance seems to follow a downstream increase, which could be attributed to the increasing number of possible point sources, or the increasing deposition of legacy sediments (Martin, 2015; Ciszewski and Grygar, 2016).

640 With regard to the floodplain cross-section patterns of plastic concentrations, no significant differentiation or lateral sorting of plastic characteristics or relationships to lateral soil texture changes were found. Here the issue arises that no previous studies have examined plastic levels in floodplain cross transects, except the study of Weber and Opp (2020), for coarse microplastics and mesoplastics, and the study of Weber et al. (2021) for medium and large microplastics in the Lahn River catchment. Both studies found a clear enrichment of plastic loads at near-channel (proximal) floodplain sites, interpreted as a consequence of

645 frequent flood occurrence at levee situations, and easier plastic retention during floods, due to higher vegetation density. In contrast, plastic loads in the Nidda floodplain seem to be much more homogeneously distributed over the floodplain area, and no differentiation based on flood dynamics and related sediment deposition occur. The slight increase of heavy metal enrichment could be traced back to the clear association of metal loads with sediment particles, reaching the floodplain when flood water overflows the riverbank (Ciszewski and Grygar, 2016). Following the diffusion mixing model, and water-flow

650 velocity slowing with increasing distance from the channel, metals associated with finer sediment fractions show higher concentrations in floodplain zones behind the levee (central, distal) (Ciszewski and Grygar, 2016). Assuming flood delivery to be the dominant source of plastic as well as heavy metal contamination, it can be stated that transport and deposition of both contaminants by floodwater is conceivable. The spatial patterns of the metal distribution correspond to well-known distribution patterns, whereas the plastic distribution shows differences to previous findings.

655 A clear and statistically significant separation of spatial patterns between the two contaminants, proved by mean differences and correlations, occurs when considering vertical distribution in floodplain soils; plastic concentrations showing a clear distinction between upper (0–50 cm) and lower (50–200 cm) soil layers (Figure 4, Figure 5). The accumulation of plastics in the uppermost topsoils, and an overall decrease in concentrations with increasing depth, was also found by the few studies that have investigated different soil depths (Liu et al., 2018; Weber and Opp, 2020), and is supported by the high levels of plastics

660 in topsoil studies (Piehl et al., 2018; Corradini et al., 2019; Christensen et al., 2020). In contrast, the recent work of Cao et al. (2021) documents renewed increases of concentration below 40 cm depth in agricultural soils. In contrast, heavy metal concentrations, which are found throughout the soil column, show significant pollution tendencies between 40 and 120 cm based on PLI, and higher enrichment below 150 cm based on EF. Assuming a more or less low mobility of heavy metals, due to good adsorption conditions in the floodplain soils examined, this pattern can probably be attributed to deposition processes

665 of heavy metals bound to sediments (Lair et al., 2009; Ciszewski and Grygar, 2016). With regard to the assumption that fluvial processes lead to the deposition and accumulation of plastics as well as heavy metals in floodplain soils, no further indicator, like a relationship to soil texture (Cao et al., 2021; Lechthaler et al., 2021), or a clear stratigraphic distinction, could be found. Nevertheless, other surface discharge pathways for microplastics, such as surface runoff on slopes, can be excluded for the studied floodplains. The direction of movement of the plastic deposits must therefore originate from the river, even if this

670 cannot be proven by data correlations or stratigraphy.

Since the vertical formation of floodplain sediments always reflects a temporal sequence of dynamic sedimentation and erosion processes, the question arises whether different time periods for the input of the two contaminants could be relevant? Although no clear temporal differentiation could be established by EPO ages, the increase in plastic concentrations between 50 and 30 cm, depending on the sampling point, suggests that deposition of plastic started at these depths, beginning in the 1950s at the

675 earliest. Assuming plastics concentration increases as a general marker for sediment dating, the upper soil layers containing significant enriched plastic concentrations could have been deposited after the 1950s (Turner et al., 2019; Weber and Lechthaler, 2021). In contrast, and although the heavy metal inputs have not stopped in recent times, deeper metal accumulations may indicate earlier impacts (e.g., mining, industry), with maximum accumulation since the 1850s, and before widespread environmental protection laws in the 1960s (Alloway, 2013). This assumption could be supported by the, in some

680 cases, strong inter-element correlations (Figure S11), indicating a combined metal pollution from similar long-term sources with the same origin and controlling factors (Manta et al., 2002; Lu and Bai, 2010).

Even though the concentrations in deeper soil layers decrease significantly, the results from the Nidda indicate that plastic particles can shift vertically, as was also shown for larger particles by Weber and Opp (2020), and smaller particles by Cao et al. (2021) and Weber et al. (2021). The size distribution of plastic particles found here, with the occurrence of coarse

685 microplastics (>2000 µm) only in upper soil layers and a considerably smaller particle size average in deep layers, suggests that smaller particles can more easily reach deeper soil sections. This result is supported by the findings of Rehm et al. (2021), showing that microplastic particles with a size of 53–100 µm tend to be carried vertically in soils more than larger particles. Possible transport paths through the soil, depending on the particle size, are assumed to be the pore space (macropores) or preferential flow paths, but also transport by soil organisms (earthworms) (Rillig et al., 2017a; Rehm et al., 2021; van Schaik

690 et al., 2014; Yu et al., 2019).

In general, it could be stated that a spatial homogenous distribution of both contaminants in floodplains exists. However, in the case of plastic contents, this only concerns the basic occurrence, since the vertical distribution is clearly influenced by the depth. Whereas the contamination of heavy metals is probably the result of multiple historic to recent sources, including point and diffuse sources, a clear source of plastic inputs is not identifiable based on this study. However, the widespread distribution

695 of plastics indicates that they can enter fluvial systems anywhere and at any time (Lechthaler et al., 2021), independent of point sources, and can accumulate temporarily in floodplains.

Despite spatial comparisons, possible interactions between plastics and heavy metals could not be identified in this study. Although the spatial differences of both contaminants were studied, no spatial or statistical correlations between plastic content and individual elements were found, which would indicate relationships like adsorption or desorption processes (Verla et al.,

700 2019). Slight negative correlation between EF and PLI values with plastic loads may indicate that adsorption of heavy metals from plastics (plastic additives) plays no role or at most a subordinate role here compared to other metal sources. Therefore, further studies should perform a targeted analysis of heavy metals on and in plastic particles, and consider geochemical interactions in addition to spatial connections.

4.4 Anthropogenic activities might directly impact distribution of plastics

Despite the general spatial distribution of plastic concentrations in floodplain soils of the Nidda River, the question arises whether there are significant outliers in the plastic concentrations and sums per site (Figure 3, Figure 4), exclusively related to the vertical distribution? Heavy metal concentrations and pollution indices show only minor outliers, which can usually be associated with individual deep-lying soil layers and single-element enrichments (Figure 8). In contrast, four significant, vertical outliers of plastic concentrations could be found in the cores NID-1, MOK-1, OKA-2 and FRA-1. Thus, at each sampling site one soil column shows a concentration of 13.86–27.25 p kg^{-1}, exceeding the average value of the respective profile by 3.3 to 6.9 times (Figure S9, Table A2). The first assumption that these enrichments are attributed to flood processes could not be confirmed, because none of the four sites has a special micro-morphology (e.g., flood channel, depression) (Figure S1) (Blettler et al., 2017; Lair et al., 2009). Also, an influence from outside the floodplain, such as slope erosion and surface flow (Rehm et al., 2021) can be excluded, since either no lower slopes are present (sites: FRA, OKA) or these are separated by roads (sites: NID, MOK).

In contrast, a relationship is evident at the OKA site between macro- and mesoplastic accumulations on the soil surface of the agricultural fields at OKA-2 (distal) as well as OKA-3 (proximal) and the enrichment of microplastic concentrations ranging between 35.82–19.39 p kg^{-1} (0–20 cm, OKA-2) or 11.44–4.93 p kg^{-1} (10–20 cm, OKA-3) in ploughed topsoil. The marked decrease of concentrations with depth could be due to compaction by tillage below the Ap horizons (Weber and Opp, 2020). Even if it is obvious to seek the source for this enrichment in agriculture, local littering cannot be ruled out. As no plasticulture was carried out on the field, the findings of macro- and mesoplastic may indicate an application of a compost or sewage sludge (functions of some plastic pieces still recognisable) (Braun et al., 2021; Steinmetz et al., 2016). However, according to information provided by the land tenant (anonymous for data protection reasons), only fertilization with manure has been carried out in recent years. Because this information is not verifiable, the entire range of possible agricultural plastic input, from fertilizer application to machine abrasion, or local littering cannot be retraced.

For the remaining enriched sites, the soil stratigraphy shows slight layer differences for the sites MOK-1 and FRA-1, but not in NID-1, and likewise without changes in soil texture. However, with consideration of land use changes (Figure S2–S3), it becomes clear that these sites were immediately adjacent to earthworks for construction purposes (bridge construction, site FRA-1) and floodplain and river restoration (sites NID-1 and MOK-1) during the 2000s and 2010s. The influence of restoration on microplastic loads in near-channel deposits, through a remobilisation of deposited plastics and a high and young sedimentary activity, was also found in the lower reaches of the Inde River (Germany) (Lechthaler et al., 2021).

Therefore, direct anthropogenic impacts like tillage and fertilization, as well as earthworks for building or restoration purposes, might have an influence on plastic content in floodplain deposits.

5. Conclusion

Floodplains and their soils can act as temporal sinks for plastics and heavy metals entering floodplain areas through flood water and flood depositions, or through agriculture. The spatially widespread and homogenous enrichment of plastics in upper floodplain soil layers indicates plastic input and distribution in fluvial systems which influences the whole floodplain soilscape. Simple interpretive hypotheses, such as increasing plastic levels with river flow following the potential increase in plastic sources, cannot be supported; rather, plastic inputs already appear to be increasing in rural and suburban areas. Furthermore, anthropogenic heavy metal enrichments, in addition to geogenic abundances, occur in the floodplain soils of the Nidda River and follow known distribution patterns resulting from fluvial transport and deposition in floodplain soils. Floodplains, as highly affected landscapes, due to their natural sink function for sediments, nutrients and pollutions, now appear to be exposed to additional contamination, resulting in a multiple contamination framework. Therefore, plastic concentrations should be included in future evaluations of floodplain conditions, ecological quality and preliminary studies for renaturation measures or construction projects.

The vertical sequence of plastic enrichment in the topsoil and upper soil layers, followed by deeper heavy metal enrichments, indicates deposition and contamination of different time periods. The floodplain soils are now contaminated with both heavy metals and plastics, although the levels are in the lower range of known concentrations in floodplain soils and soils in general. However, since the environmental impacts and consequences for humans of plastic contamination in soils, are still not entirely understood, even low levels of accumulation should not be ignored. Not least because a further increase in plastic production, and thus, an increase in plastic emissions into the environment, can be expected. Further areal and spatially representative monitoring of plastic contents in soils, their input pathways, and the investigation of possible interrelationships with other pollutants, will be necessary in the future in order to provide risk assessments in case of upcoming legislation.

Finally, direct short and long-term anthropogenic impacts, like tillage and probably soil fertilization, as well as earthworks and floodplain restoration could affect plastic enrichment. While agriculture and tillage can be interpreted as an emitting and spreading agent, earthworks and renaturation could be seen as redistributing agents for plastic deposits. Against the background of the manifold conflicts of use in floodplains, and the increasing renaturation and withdrawal of watercourse structures for nature conservation and flood protection purposes, the question arises as to whether these measures encourage the temporary storage of plastics in floodplain soils? Relocation of legacy sediments, increase in erosion due to channel relocation, or removal of bank stabilisers, could result in renewed plastic discharges, resulting in further inputs into aquatic and marine ecosystems that are already severely affected by plastic contaminations.

Based on our case study, the methodological limitations and our findings, the following recommendations can be made for further research and the management of floodplains:

- Multiple plastic monitoring in soils should be carried out in a spatially representative manner. Those studies can contribute to the understanding of interrelationships and influences across soilscapes, improve knowledge of sources and transport routes, and implement targeted containment measures in the future.

- Standardisation of analysis methods, in order to develop a reliable and comparable database. Should plastic be recognised as a pollutant at the legislative level, uniform assessment data must be obtained for risk assessment and
770 policy development.

- Plastic levels in soils should be considered in construction and landscape planning. In terms of precautionary soil protection, consideration should be given to the consequences of anthropogenic interventions such as renaturation on the storage or discharge of plastics.

- Ultimately, precautions must be taken to limit plastic input into the environment, regardless of the source. This
775 frequently formulated demand includes the transition to an efficient circular economy as well as further public relations work.

780

785

790 **Appendices**

SOIL Discussions | Open Access | EGU

Table A 1: Sampling site features with soil and soilscape properties.

Tran-sect sites	Catchment properties			Sampling points	Floodplain properties			Soil properties			Soilscape description
	Catchment zone	River km[a]	Flood area (m)[a]		Morphological unit	Land use	Channel distance (m)	Soil type (WRB[b])	Horizon frequence[c]	Soil textures	
NID	upper middle reaches	62.5	520.5	NID-1	back swamp	grassland	447.9	Fluvic **Gleysol** (Clayic)	Ahl-Bl-Br	SiCL and SiC	Very fine-grained fluvial soils under strong groundwater influence and enrichment of limnic layers (peat)
				NID-2	riparian plane	grassland	35.5	Endogleyic **Fluvisol** (Siltic, Clayic, Limnic)	Ah-B-Bl-Blr-Br-Lhr	SiL and SiC	
MOK	middle reaches	55.0	861.2	MOK-1	back swamp	grassland	859.7	Fluvic **Gleysol** (Siltic, Limnic)	Ahl-Blr-Br-Lhr	SiC and C	Fine-grained fluvial soils under groundwater and stagnig surface water influence and partial enrichment of limnic layers
				MOK-2	plane	grassland	467.0	Endogleyic, Endostagnic **Fluvisol** (Siltic, Limnic)	Ahg-Bgl-Bgr-Br-Lr	SiC and C	
				MOK-3	riparian	grassland	28.4	Epigleyic **Fluvisol** (Siltic)	Ah-B-Bl-Blr-Br	SiL	
OKA	upper lower reaches	35.5	777.5	OKA-1	back swamp	grassland	532.2	Endogleyic, Endostagnic **Fluvisol** (Siltic)	Ah-Bgl-Blr-Br	SiCL and SiC	Fine-grained fluvial soils under groundwater and stagnig surface water influence with partial anthropogenic influence (artefacts)
				OKA-2	plane	cropland	315.2	**Fluvisol** (Antric, Siltic)	Ap-B-Bgu-Bl-Blr	SiCL and SiL	
				OKA-3	riparian	cropland	23.0	**Fluvisol** (Antric, Siltic)	Ap-B-Bl-Br	SiL and SiC	
FRA	lower reach	2.0	427.0	FRA-2	plane	grassland	203.4	Endogleyic **Fluvisol** (Silitc)	Ah-Apb-B-Bl-Brl-Br	SiL and SL	Fine-grained fluvial soils partial under groundwater influence and strong anthropogenic urban influence
				FRA-1	plane	grassland	21.4	Fluvisol (Silitc)	Ah-B-Bl-Blr-Br	SiL	

[a] according to WRRL-Viewer Hesse (2021); [b] World Reference Base for Soil Resources (2015); [c] according to Guidelines for soil description (FAO, 2006); [d] according to the soil profiles presented here and preliminary survey of the wider sampling site environment

795

Table A 2: Average contents of plastic abundance, selected elements, pollution indices and soil conditions within studied soil profiles.

Transect (*river km*)	Sampling point	Average plastic load (p kg^{-1})	Elemental contents (mg kg^{-1})[a]						Pollution indices		Soil conditions				
			Cr	Ni	Cu	Zn	Cd	Pb	EF[b]	PLI[c]	Clay[d]	Silt[d]	Sand[d]	OM[e]	pH
NID (*62.5 km*)	NID-1	3.92	21.77	24.73	14.00	45.47	0.26	24.22	2.54	0.99	41.0	52.9	6.1	10.1	5.8
	NID-2	3.92	29.54	29.50	16.66	50.76	0.21	21.11	2.30	1.01	33.3	62.0	4.7	9.3	6.0
MOK (*55.0 km*)	MOK-1	4.19	32.38	31.50	18.34	68.39	0.43	29.19	2.54	1.29	47.9	47.0	5.1	14.5	6.4
	MOK-2	1.06	37.61	42.73	24.24	83.01	0.45	34.46	2.56	1.54	46.7	45.1	8.2	11.5	5.5
	MOK-3	1.78	26.66	28.71	14.77	55.83	0.32	24.07	2.23	0.87	22.1	67.8	10.1	6.2	5.9
OKA (*35.5 km*)	OKA-1	1.73	27.39	28.41	15.20	49.74	0.22	19.79	2.05	0.98	28.3	49.7	22.0	7.6	6.9
	OKA-2	6.44	33.88	33.03	16.52	55.41	0.25	20.93	2.27	1.11	30.6	58.7	10.7	7.7	7.3
	OKA-3	2.22	32.72	36.64	18.36	55.38	0.25	22.74	1.86	1.28	31.5	58.9	9.6	6.5	6.7
FRA (*2.0 km*)	FRA-2	2.85	28.98	26.76	13.21	42.41	0.17	19.82	1.91	0.89	19.1	50.4	30.5	4.6	6.1
	FRA-1	4.19	28.02	30.85	15.29	50.66	0.27	22.50	2.03	1.01	19.5	59.7	20.8	5.4	6.9

[a] Average values of selected elements according to existing precautionary values in the German Federal Soil Protection Ordinance; [b] Enrichment factor (>2 = moderate enrichment); [c] Pollution load index (> 1 = significant pollution); [d] Grain size composition given in mass percent (wt%); [e] Organic matter given in mass percent (wt%).

SOIL
Discussions

Open Access

EGU

Data availability

The complete dataset that was gathered within the framework of the present study is freely accessible at the following repository: Collin J. Weber (2022): Meso- and microplastic distribution and heavy metal contaminations in floodplains of the Nidda River (Germany) available under 10.6084/m9.figshare.17714909

815 **Author contribution**

Conceptualisation, C.J.W. and C.O.; Methodology, C.J.W. and J.A.P.; Validation, C.J.W.; Formal Analyses, C.J.W.; Investigation, C.J.W.; Resources, C.J.W., C.O., M.K. and P.C.; Data Curation, C.J.W., Writing – Original Draft, C.J.W., Writing – Review & Editing, C.J.W., C.O., J.A.P. and M.K., Visualisation, C.J.W.; Supervision, C.O., M.K. and P.C.; Project Administration, C.J.W.; Funding Acquisition, C.J.W. and C.O.

820 **Competing interests**

The authors declare that they have no conflict of interest.

Acknowledgements

References

Ad-hoc AG Boden: Bodenkundliche Kartieranleitung, 5th ed., Schweizerbart, Stuttgart, 438 S, 2005.

Alloway, B. J.: Heavy Metals in Soils, 22, Springer Netherlands, Dordrecht, 614 pp., 2013.

830 Andrady, A. L.: The plastic in microplastics: A review, Marine Pollution Bulletin, 119, 12–22, https://doi.org/10.1016/j.marpolbul.2017.01.082, 2017.

Bancone, C. E. P., Turner, S. D., Ivar do Sul, J. A., and Rose, N. L.: The Paleoecology of Microplastic Contamination, Front. Environ. Sci., 8, https://doi.org/10.3389/fenvs.2020.574008, 2020.

Blettler, M. C. M., Ulla, M. A., Rabuffetti, A. P., and Garello, N.: Plastic pollution in freshwater ecosystems: macro-, meso-,
835   and microplastic debris in a floodplain lake, Environmental monitoring and assessment, 189, 581,
https://doi.org/10.1007/s10661-017-6305-8, 2017.

Blume, H.-P., Brümmer, G. W., Fleige, H., Horn, R., Kandeler, E., Kögel-Knabner, I., Kretzschmar, R., Stahr, K., and
Wilke, B.-M.: Scheffer/Schachtschabel Soil Science, Springer Berlin Heidelberg, Berlin, Heidelberg, s.l., 618 pp., 2016.

Braun, M., Mail, M., Heyse, R., and Amelung, W.: Plastic in compost: Prevalence and potential input into agricultural and
840   horticultural soils, The Science of the Total Environment, 760, 143335, https://doi.org/10.1016/j.scitotenv.2020.143335,
2021.

Brettschneider, D. J., Misovic, A., Schulte-Oehlmann, U., Oetken, M., and Oehlmann, J.: Detection of chemically induced
ecotoxicological effects in rivers of the Nidda catchment (Hessen, Germany) and development of an ecotoxicological,
Water Framework Directive–compliant assessment system, Environ Sci Eur, 31, https://doi.org/10.1186/s12302-019-
845   0190-4, 2019.

Bundesregierung: Bundes-Bodenschutz- und Altlastenverordnung: BBodSchV, 1998.

Calmano, W., Hong, J., and Förstner, U.: Binding and mobilization of heavy metals in contaminated sediments affected by
pH and redox potential, Water Science & Technology, 223–235, 1993.

Cao, L., Di Wu, Liu, P., Hu, W., Xu, L., Sun, Y., Wu, Q., Tian, K., Huang, B., Yoon, S. J., Kwon, B.-O., and Khim, J. S.:
850   Occurrence, distribution and affecting factors of microplastics in agricultural soils along the lower reaches of Yangtze
River, China, The Science of the Total Environment, 794, 148694, https://doi.org/10.1016/j.scitotenv.2021.148694,
2021.

Catrouillet, C., Davranche, M., Khatib, I., Fauny, C., Wahl, A., and Gigault, J.: Metals in microplastics: determining which
are additive, adsorbed, and bioavailable, Environ. Sci.: Processes Impacts, 23, 553–558,
855   https://doi.org/10.1039/D1EM00017A, 2021.

Chamas, A., Moon, H., Zheng, J., Qiu, Y., Tabassum, T., Jang, J. H., Abu-Omar, M., Scott, S. L., and Suh, S.: Degradation
Rates of Plastics in the Environment, ACS Sustainable Chem. Eng., 8, 3494–3511,
https://doi.org/10.1021/acssuschemeng.9b06635, 2020.

Christensen, N. D., Wisinger, C. E., Maynard, L. A., Chauhan, N., Schubert, J. T., Czuba, J. A., and Barone, J. R.: Transport
860   and characterization of microplastics in inland waterways, Journal of Water Process Engineering, 38, 101640,
https://doi.org/10.1016/j.jwpe.2020.101640, 2020.

Ciszewski, D. and Grygar, T. M.: A Review of Flood-Related Storage and Remobilization of Heavy Metal Pollutants in
River Systems, Water Air Soil Pollut, 227, 239, https://doi.org/10.1007/s11270-016-2934-8, 2016.

Corradini, F., Meza, P., Eguiluz, R., Casado, F., Huerta-Lwanga, E., and Geissen, V.: Evidence of microplastic accumulation
865   in agricultural soils from sewage sludge disposal, The Science of the Total Environment, 671, 411–420,
https://doi.org/10.1016/j.scitotenv.2019.03.368, 2019.

Cutroneo, L., Reboa, A., Geneselli, I., and Capello, M.: Considerations on salts used for density separation in the extraction of microplastics from sediments, Marine Pollution Bulletin, 166, 112216, https://doi.org/10.1016/j.marpolbul.2021.112216, 2021.

870 D'Elia, A. H., Liles, G. C., Viers, J. H., and Smart, D. R.: Deep carbon storage potential of buried floodplain soils, Scientific reports, 7, 8181, https://doi.org/10.1038/s41598-017-06494-4, 2017.

Dong, M., Luo, Z., Jiang, Q., Xing, X., Zhang, Q., and Sun, Y.: The rapid increases in microplastics in urban lake sediments, Scientific reports, 10, 848, https://doi.org/10.1038/s41598-020-57933-8, 2020.

Dudka, S. and Adriano, D. C.: Environmental impacts of metal ore mining and processing: A review, J. Environ. Qual.,
875 1997, 590–602, https://doi.org/10.2134/jeq1997.00472425002600030003x, 1997.

Durner, W., Iden, S. C., and Unold, G. von: The integral suspension pressure method (ISP) for precise particle-size analysis by gravitational sedimentation, Water Resour. Res., 53, 33–48, https://doi.org/10.1002/2016WR019830, 2017.

Edgeworth, M.: Fluid Pasts - Archaeology of flow, Bristol Classical Press, London, 2011.

FAO: Guidelines for soil description, 4th ed., Food and Agriculture Organization of the United Nations, Rome, x, 97, 2006.

880 Friedrich, K. and Lügger, K.: Hintergrundwerte von Spurenstoffen in hessischen Böden, Hessian Agency of Nature Conservation, Environment and Geology (HLNUG), Wiesbaden, 2011.

Hahladakis, J. N., Velis, C. A., Weber, R., Iacovidou, E., and Purnell, P.: An overview of chemical additives present in plastics: Migration, release, fate and environmental impact during their use, disposal and recycling, Journal of Hazardous Materials, 344, 179–199, https://doi.org/10.1016/j.jhazmat.2017.10.014, 2018.

885 Hahn, J., Opp, C., Zitzer, N., and Laufenberg, G.: Impacts of river impoundment on dissolved heavy metals in floodplain soils of the Lahn River (Germany), Environ Earth Sci, 75, https://doi.org/10.1007/s12665-016-5950-5, 2016.

Hartmann, N. B., Hüffer, T., Thompson, R. C., Hassellöv, M., Verschoor, A., Daugaard, A. E., Rist, S., Karlsson, T., Brennholt, N., Cole, M., Herrling, M. P., Hess, M. C., Ivleva, N. P., Lusher, A. L., and Wagner, M.: Are We Speaking the Same Language? Recommendations for a Definition and Categorization Framework for Plastic Debris, Environ. Sci.
890 Technol., 53, 1039–1047, https://doi.org/10.1021/acs.est.8b05297, 2019.

He, B., Smith, M., Egodawatta, P., Ayoko, G. A., Rintoul, L., and Goonetilleke, A.: Dispersal and transport of microplastics in river sediments, Environmental Pollution, 279, 116884, https://doi.org/10.1016/j.envpol.2021.116884, 2021.

Hessian State Statistical Office: Hessische Gemeindestatistik, Gemeinden in Hessen [Hessian Municipal Statistics, Municipalities in Hesse, in German], https://statistik.hessen.de/publikationen/thematische-
895 veroeffentlichungen/gemeinden-hessen, last access: 3 August 2021, 2021.

Hidalgo-Ruz, V., Gutow, L., Thompson, R. C., and Thiel, M.: Microplastics in the marine environment: a review of the methods used for identification and quantification, Environmental Science & Technology, 46, 3060–3075, https://doi.org/10.1021/es2031505, 2012.

Holmes, L. A., Turner, A., and Thompson, R. C.: Adsorption of trace metals to plastic resin pellets in the marine
900 environment, Environmental Pollution, 160, 42–48, https://doi.org/10.1016/j.envpol.2011.08.052, 2012.

Huerta Lwanga, E., Mendoza Vega, J., Ku Quej, V., Chi, J. d. L. A., Sanchez Del Cid, L., Chi, C., Escalona Segura, G., Gertsen, H., Salánki, T., van der Ploeg, M., Koelmans, A. A., and Geissen, V.: Field evidence for transfer of plastic debris along a terrestrial food chain, Scientific reports, 7, 14071, https://doi.org/10.1038/s41598-017-14588-2, 2017.

Hürkamp, K., Raab, T., and Völkel, J.: Lead Pollution of Floodplain Soils in a Historic Mining Area—Age, Distribution and Binding Forms, Water Air Soil Pollut, 201, 331–345, https://doi.org/10.1007/s11270-008-9948-9, 2009.

Hurley, R., Woodward, J., and Rothwell, J. J.: Microplastic contamination of river beds significantly reduced by catchment-wide flooding, Nat. Geosci., 11, 251–257, https://doi.org/10.1038/s41561-018-0080-1, 2018.

Imhof, H. K., Schmid, J., Niessner, R., Ivleva, N. P., and Laforsch, C.: A novel, highly efficient method for the separation and quantification of plastic particles in sediments of aquatic environments, Limnol. Oceanogr. Methods, 10, 524–537, https://doi.org/10.4319/lom.2012.10.524, 2012.

International Organization for Standardization: Plastics — Environmental aspects — State of knowledge and methodologies, available at: https://www.iso.org/obp/ui/#iso:std:iso:tr:21960:ed-1:v1:en, 2020.

IUSS Working Group: World reference base for soil resources 2014, update 2015: International soil classification system for naming soils and creating legends for soil maps, World Soil Resources Reports, FAO, 2015.

Jockenhövel, A.: Die Jungsteinzeit [Early Neolithic, in German], in: Die Vorgeschichte Hessens [The Prehistory of Hesse, in German], edited by: Jockenhövel, H., Theiss, Stuttgart, 121–194, 1990.

Jung, M. R., Horgen, F. D., Orski, S. V., Rodriguez C, V., Beers, K. L., Balazs, G. H., Jones, T. T., Work, T. M., Brignac, K. C., Royer, S.-J., Hyrenbach, K. D., Jensen, B. A., and Lynch, J. M.: Validation of ATR FT-IR to identify polymers of plastic marine debris, including those ingested by marine organisms, Marine Pollution Bulletin, 127, 704–716, https://doi.org/10.1016/j.marpolbul.2017.12.061, 2018.

Kabata-Pendias, A.: Trace elements in soils and plants, 4. ed., CRC Press, Boca Raton, Fla., 520 pp., 2011.

Karbalaei, S., Hanachi, P., Walker, T. R., and Cole, M.: Occurence, sources, human health impacts and mitigation of microplastic pollution, Environmental Science and Pollution Research, 36046–36063, https://doi.org/10.1007/s11356-018-3508-7, 2018.

Kern, O. A., Koutsodendris, A., Süfke, F., Gutjahr, M., Mächtle, B., and Pross, J.: Persistent, multi-sourced lead contamination in Central Europe since the Bronze Age recorded in the Füramoos peat bog, Germany, Anthropocene, 36, 100310, https://doi.org/10.1016/j.ancene.2021.100310, 2021.

Kiss, T., Fórián, S., Szatmári, G., and Sipos, G.: Spatial distribution of microplastics in the fluvial sediments of a transboundary river - A case study of the Tisza River in Central Europe, The Science of the Total Environment, 785, 147306, https://doi.org/10.1016/j.scitotenv.2021.147306, 2021.

Klein, S., Worch, E., and Knepper, T. P.: Occurrence and Spatial Distribution of Microplastics in River Shore Sediments of the Rhine-Main Area in Germany, Environmental Science & Technology, 49, 6070–6076, https://doi.org/10.1021/acs.est.5b00492, 2015.

905

910

915

920

925

930

Konde, S., Ornik, J., Prume, J. A., Taiber, J., and Koch, M.: Exploring the potential of photoluminescence spectroscopy in
935   combination with Nile Red staining for microplastic detection, Marine Pollution Bulletin, 159, 111475,
     https://doi.org/10.1016/j.marpolbul.2020.111475, available at:
     http://www.sciencedirect.com/science/article/pii/S0025326X20305932, 2020.

Kooi, M. and Koelmans, A. A.: Simplifying Microplastic via Continuous Probability Distributions for Size, Shape, and
     Density, Environ. Sci. Technol. Lett., 6, 551–557, https://doi.org/10.1021/acs.estlett.9b00379, 2019.

940 Kowalska, J. B., Mazurek, R., Gąsiorek, M., and Zaleski, T.: Pollution indices as useful tools for the comprehensive
     evaluation of the degree of soil contamination-A review, Environmental geochemistry and health, 40, 2395–2420,
     https://doi.org/10.1007/s10653-018-0106-z, 2018.

Kühn, P., Lehndorff, E., and Fuchs, M.: Lateglacial to Holocene pedogenesis and formation of colluvial deposits in a loess
     landscape of Central Europe (Wetterau, Germany), Catena, 154, 118–135, https://doi.org/10.1016/j.catena.2017.02.015,
945   2017.

Lair, G. J., Zehetner, F., Fiebig, M., Gerzabek, M. H., van Gestel, C. A. M., Hein, T., Hohensinner, S., Hsu, P., Jones, K. C.,
     Jordan, G., Koelmans, A. A., Poot, A., Slijkerman, D. M. E., Totsche, K. U., Bondar-Kunze, E., and Barth, J. A. C.:
     How do long-term development and periodical changes of river-floodplain systems affect the fate of contaminants?
     Results from European rivers, Environmental Pollution, 157, 3336–3346, https://doi.org/10.1016/j.envpol.2009.06.004,
950   2009.

Lang, A. and Nolte, S.: The chronology of Holocene alluvial sediments from the Wetterau, Germany, provided by optical
     and 14C dating, The Holocene, 207–214, https://doi.org/10.1191/2F095968399675119300, 1999.

Lechthaler, S., Esser, V., Schüttrumpf, H., and Stauch, G.: Why analysing microplastics in floodplains matters: application
     in a sedimentary context, Environ. Sci.: Processes Impacts, 71, 299, https://doi.org/10.1039/D0EM00431F, 2021.

955 Lechthaler, S., Waldschläger, K., Stauch, G., and Schüttrumpf, H.: The Way of Macroplastic through the Environment,
     Environments, 7, 73, https://doi.org/10.3390/environments7100073, 2020.

Liu, M., Lu, S., Song, Y., Lei, L., Hu, J., Lv, W., Zhou, W., Cao, C., Shi, H., Yang, X., and He, D.: Microplastic and
     mesoplastic pollution in farmland soils in suburbs of Shanghai, China, Environmental Pollution, 242, 855–862,
     https://doi.org/10.1016/j.envpol.2018.07.051, 2018.

960 Lu, S. G. and Bai, S. Q.: Contamination and potential mobility assessment of heavy metals in urban soils of Hangzhou,
     China: relationship with different land uses, Environ Earth Sci, 60, 1481–1490, https://doi.org/10.1007/s12665-009-
     0283-2, 2010.

Maes, T., Jessop, R., Wellner, N., Haupt, K., and Mayes, A.G.: A rapid-screening approach to detect and quantify
     microplastics based in fluorescent tagging with Nile Red, Scientific reports, https://doi.org/10.1038/srep44501, 2017.

965 Manta, D. S., Angelone, M., Bellanca, A., Neri, R., and Sprovieri, M.: Heavy metals in urban soils: a case study from the
     city of Palermo (Sicily), Italy, Science of The Total Environment, 300, 229–243, https://doi.org/10.1016/S0048-
     9697(02)00273-5, 2002.

SOIL
Discussions
Open Access
EGU

Martin, C. W.: Trace metal storage in recent floodplain sediments along the Dill River, central Germany, Geomorphology, 235, 52–62, https://doi.org/10.1016/j.geomorph.2015.01.032, 2015.

970   Martin, C. W.: Recent changes in heavy metal contamination at near-channel positions of the Lahn River, central Germany, Geomorphology, 139-140, 452–459, https://doi.org/10.1016/j.geomorph.2011.11.010, 2012.

Möller, J. N., Löder, M. G. J., and Laforsch, C.: Finding Microplastics in Soils: A Review of Analytical Methods, Environ. Sci. Technol., 54, 2078–2090, https://doi.org/10.1021/acs.est.9b04618, 2020.

Munier, B. and Bendell, L. I.: Macro and micro plastics sorb and desorb metals and act as a point source of trace metals to

975   coastal ecosystems, PloS one, 13, e0191759, https://doi.org/10.1371/journal.pone.0191759, 2018.

Napper, I. E. and Thompson, R. C.: Environmental Deterioration of Biodegradable, Oxo-biodegradable, Compostable, and Conventional Plastic Carrier Bags in the Sea, Soil, and Open-Air Over a 3-Year Period, Environmental Science & Technology, 4775–4783, https://doi.org/10.1021/acs.est.8b06984, 2019.

Nardi, F., Annis, A., Di Baldassarre, G., Vivoni, E. R., and Grimaldi, S.: GFPLAIN250m, a global high-resolution dataset of

980   Earth's floodplains, Scientific data, 6, 180309, https://doi.org/10.1038/sdata.2018.309, 2019.

Noren, F.: Small plastic particles in Coastal Swedish waters, KIMO Sweden, 2012.

Opp, C., Stach, J. and Hanschmann, G.: Load on differently used soils by heavy metals within the highly contaminated area of Bitterfeld (FRG). The Science of the Total Environment, 134, 141-150, 1993

Pejman, A., Nabi Bidhendi, G., Ardestani, M., Saeedi, M., and Baghvand, A.: A new index for assessing heavy metals

985   contamination in sediments: A case study, Ecological Indicators, 58, 365–373, https://doi.org/10.1016/j.ecolind.2015.06.012, 2015.

Piehl, S., Leibner, A., Löder, M. G. J., Dris, R., Bogner, C., and Laforsch, C.: Identification and quantification of macro- and microplastics on an agricultural farmland, Scientific reports, 8, 17950, https://doi.org/10.1038/s41598-018-36172-y, 2018.

990   PlasticsEurope: Plastics - the facts 2020: An analysis of European plastic production, demand and waste data, available at: https://www.plasticseurope.org/en/resources/publications/4312-plastics-facts-2020, 2020.

PlasticsEurope: Plastics - the facts 2018: An analysis of European plastic production, demand and waste data, Plastic Europe, available at: https://www.plasticseurope.org/download_file/force/2387/319, 2018.

Price, S. J., Ford, J. R., Cooper, A. H., and Neal, C.: Humans as major geological and geomorphological agents in the

995   Anthropocene: the significance of artificial ground in Great Britain, Philosophical transactions. Series A, Mathematical, physical, and engineering sciences, 369, 1056–1084, https://doi.org/10.1098/rsta.2010.0296, 2011.

Primpke, S., Lorenz, C., Rascher-Friesenhausen, R., and Gerdts, G.: An automated approach for microplastics analysis using focal plane array (FPA) FTIR microscopy and image analysis, Anal. Methods, 9, 1499–1511, https://doi.org/10.1039/C6AY02476A, 2017.

1000 Primpke, S., Wirth, M., Lorenz, C., and Gerdts, G.: Reference database design for the automated analysis of microplastic samples based on Fourier transform infrared (FTIR) spectroscopy, Analytical and Bioanalytical Chemistry, 410, 5131–5141, https://doi.org/10.1007/s00216-018-1156-x, 2018.

Prume, J. A., Gorka, F., and Löder, M. G.: From sieve to microscope: An efficient technique for sample transfer in the process of microplastics' quantification, MethodsX, 8, 101341, https://doi.org/10.1016/j.mex.2021.101341, 2021.

1005 Qi, R., Jones, D. L., Li, Z., Liu, Q., and Yan, C.: Behavior of microplastics and plastic film residues in the soil environment: A critical review, The Science of the Total Environment, 703, 134722, https://doi.org/10.1016/j.scitotenv.2019.134722, 2020.

Ragusa, A., Svelato, A., Santacroce, C., Catalano, P., Notarstefano, V., Carnevali, O., Papa, F., Rongioletti, M. C. A., Baiocco, F., Draghi, S., D'Amore, E., Rinaldo, D., Matta, M., and Giorgini, E.: Plasticenta: First evidence of
1010 microplastics in human placenta, Environment International, 146, 106274, https://doi.org/10.1016/j.envint.2020.106274, 2021.

Regional Council Darmstadt: Flood risk management plan for the water system of the river Nidda (in German), Regional Council Darmstadt, Darmstadt, 2015.

Rehm, R., Zeyer, T., Schmidt, A., and Fiener, P.: Soil erosion as transport pathway of microplastic from agriculture soils to
1015 aquatic ecosystems, The Science of the Total Environment, 795, 148774, https://doi.org/10.1016/j.scitotenv.2021.148774, 2021.

Rillig, M. C., Lehmann, A., Souza Machado, A. A. de, and Yang, G.: Microplastic effects on plants, The New phytologist, https://doi.org/10.1111/nph.15794, 2019.

Rillig, M. C., Ziersch, L., and Hempel, S.: Microplastic transport in soil by earthworms, Scientific reports, 7, 1362,
1020 https://doi.org/10.1038/s41598-017-01594-7, 2017a.

Rillig, M. C., Ingraffia, R., and Souza Machado, A. A. de: Microplastic Incorporation into Soil in Agroecosystems, Frontiers in plant science, 8, 1805, https://doi.org/10.3389/fpls.2017.01805, 2017b.

Scheurer, M. and Bigalke, M.: Microplastics in Swiss Floodplain Soils, Environmental Science & Technology, 52, 3591–3598, https://doi.org/10.1021/acs.est.7b06003, 2018.

1025 Schmidt, K., Behrens, T., Friedrich, K., and Scholten, T.: A method to generate soilscapes from soil maps, Z. Pflanzenernähr. Bodenk., 173, 163–172, https://doi.org/10.1002/jpln.200800208, 2010.

Schweizer, M., Dieterich, A., Corral Morillas, N., Dewald, C., Miksch, L., Nelson, S., Wick, A., Triebskorn, R., and Köhler, H.-R.: The importance of sediments in ecological quality assessment of stream headwaters: embryotoxicity along the Nidda River and its tributaries in Central Hesse, Germany, Environ Sci Eur, 30, 22, https://doi.org/10.1186/s12302-018-
1030 0150-4, 2018.

Selonen, S., Dolar, A., Jemec Kokalj, A., Skalar, T., Parramon Dolcet, L., Hurley, R., and van Gestel, C. A. M.: Exploring the impacts of plastics in soil - The effects of polyester textile fibers on soil invertebrates, The Science of the Total Environment, 700, 134451, https://doi.org/10.1016/j.scitotenv.2019.134451, 2020.

Siegfried, M., Koelmans, A. A., Besseling, E., and Kroeze, C.: Export of microplastics from land to sea. A modelling approach, Water research, 127, 249–257, https://doi.org/10.1016/j.watres.2017.10.011, 2017.

Souza Machado, A. A. de, Lau, C. W., Till, J., Kloas, W., Lehmann, A., Becker, R., and Rillig, M. C.: Impacts of Microplastics on the Soil Biophysical Environment, Environ. Sci. Technol., 52, 9656–9665, https://doi.org/10.1021/acs.est.8b02212, 2018.

Steinmetz, Z., Wollmann, C., Schaefer, M., Buchmann, C., David, J., Tröger, J., Muñoz, K., Frör, O., and Schaumann, G. E.: Plastic mulching in agriculture. Trading short-term agronomic benefits for long-term soil degradation?, The Science of the Total Environment, 550, 690–705, https://doi.org/10.1016/j.scitotenv.2016.01.153, 2016.

Thomas, R.: A Beginner's Guide to ICP-MS, Spectroscopy, 16, https://www.spectroscopyonline.com/view/challenges-of-spectrofluorometry-part-1-collect-data-right-the-first-time, 2001.

Turner, S., Horton, A. A., Rose, N. L., and Hall, C.: A temporal sediment record of microplastics in an urban lake, London, UK, J Paleolimnol, 61, 449–462, https://doi.org/10.1007/s10933-019-00071-7, 2019.

van Schaik, L., Palm, J., Klaus, J., Zehe, E., and Schröder, B.: Linking spatial earthworm distribution to macropore numbers and hydrological effectiveness, Ecohydrol., 7, 401–408, https://doi.org/10.1002/eco.1358, 2014.

Verla, A. W., Enyoh, C. E., Verla, E. N., and Nwarnorh, K. O.: Microplastic–toxic chemical interaction: a review study on quantified levels, mechanism and implication, SN Appl. Sci., 1, 339, https://doi.org/10.1007/s42452-019-1352-0, 2019.

Voica, C., Dehelean, A., Iordache, A., and Geana, I.: Method validation for determination of metals in soils by ICP-MS, Romanian Reports in Physics, 221–231, 2012.

Wang, J., Liu, X., Li, Y., Powell, T., Wang, X., Wang, G., and Zhang, P.: Microplastics as contaminants in the soil environment: A mini-review, The Science of the Total Environment, 691, 848–857, https://doi.org/10.1016/j.scitotenv.2019.07.209, 2019.

Wang, W., Ge, J., Yu, X., and Li, H.: Environmental fate and impacts of microplastics in soil ecosystems: Progress and perspective, The Science of the Total Environment, 708, 134841, https://doi.org/10.1016/j.scitotenv.2019.134841, 2020.

Waters, C. N., Zalasiewicz, J., Summerhayes, C., Barnosky, A. D., Poirier, C., Gałuszka, A., Cearreta, A., Edgeworth, M., Ellis, E. C., Ellis, M., Jeandel, C., Leinfelder, R., McNeill, J. R., Richter, D. d., Steffen, W., Syvitski, J., Vidas, D., Wagreich, M., Williams, M., an Zhisheng, Grinevald, J., Odada, E., Oreskes, N., and Wolfe, A. P.: The Anthropocene is functionally and stratigraphically distinct from the Holocene, Science (New York, N.Y.), 351, aad2622, https://doi.org/10.1126/science.aad2622, 2016.

Weber, C. J. and Lechthaler, S.: Plastics as a stratigraphic marker in fluvial deposits, Anthropocene, 36, 100314, https://doi.org/10.1016/j.ancene.2021.100314, 2021.

Weber, C. J., Opp, C., Prume, J. A., Koch, M., Andersen, T. J. and Chifflard, P.: Deposition and in-situ translocation of microplastics in floodplain soils, The Science of the Total Environment, 102539, https://doi.org/10.1016/j.scitotenv.2021.152039, 2021.

Weber, C. J. and Opp, C.: Spatial patterns of mesoplastics and coarse microplastics in floodplain soils as resulting from land use and fluvial processes, Environmental Pollution, 267, 115390, https://doi.org/10.1016/j.envpol.2020.115390, 2020.

Weihrauch, C.: Dynamics need space – A geospatial approach to soil phosphorus' reactions and migration, Geoderma, 354, 113775, https://doi.org/10.1016/j.geoderma.2019.05.025, 2019.

Weihrauch, C. and Weber, C. J.: Phosphorus enrichment in floodplain subsoils as a potential source of freshwater eutrophication, The Science of the Total Environment, 747, 141213, https://doi.org/10.1016/j.scitotenv.2020.141213, 2020.

Xiong, X., Wu, C., Elser, J. J., Mei, Z., and Hao, Y.: Occurrence and fate of microplastic debris in middle and lower reaches of the Yangtze River - From inland to the sea, The Science of the Total Environment, 659, 66–73, https://doi.org/10.1016/j.scitotenv.2018.12.313, 2018.

Yu, H., Zhang, Z., Zhang, Y., Fan, P., Xi, B., and Tan, W.: Metal type and aggregate microenvironment govern the response sequence of speciation transformation of different heavy metals to microplastics in soil, The Science of the Total Environment, 752, 141956, https://doi.org/10.1016/j.scitotenv.2020.141956, 2021.

Yu, H., Hou, J., Dang, Q., Cui, D., Xi, B., and Tan, W.: Decrease in bioavailability of soil heavy metals caused by the presence of microplastics varies across aggregate levels, Journal of Hazardous Materials, 395, 122690, https://doi.org/10.1016/j.jhazmat.2020.122690, 2020.

Yu, M., van der Ploeg, M., Lwanga, E. H., Yang, X., Zhang, S., Ma, X., Ritsema, C. J., and Geissen, V.: Leaching of microplastics by preferential flow in earthworm (Lumbricus terrestris) burrows, Environ. Chem., 16, 31, https://doi.org/10.1071/EN18161, 2019.

Zalasiewicz, J., Waters, C. N., Ellis, E. C., Head, M. J., Vidas, D., Steffen, W., Thomas, J. A., Horn, E., Summerhayes, C. P., Leinfelder, R., McNeill, J. R., Gałuszka, A., Williams, M., Barnosky, A. D., Richter, D. d. B., Gibbard, P. L., Syvitski, J., Jeandel, C., Cearreta, A., Cundy, A. B., Fairchild, I. J., Rose, N. L., Ivar do Sul, J. A., Shotyk, W., Turner, S., Wagreich, M., and Zinke, J.: The Anthropocene: Comparing Its Meaning in Geology (Chronostratigraphy) with Conceptual Approaches Arising in Other Disciplines, Earth's Future, 9, https://doi.org/10.1029/2020EF001896, 2021.

Zalasiewicz, J., Waters, C. N., Ivar do Sul, J. A., Corcoran, P. L., Barnosky, A. D., Cearreta, A., Edgeworth, M., Gałuszka, A., Jeandel, C., Leinfelder, R., McNeill, J. R., Steffen, W., Summerhayes, C., Wagreich, M., Williams, M., Wolfe, A. P., and Yonan, Y.: The geological cycle of plastics and their use as a stratigraphic indicator of the Anthropocene, Anthropocene, 13, 4–17, https://doi.org/10.1016/j.ancene.2016.01.002, 2016.

Zhang, B., Yang, X., Chen, L., Chao, J., Teng, J., and Wang, Q.: Microplastics in soils: a review of possible sources, analytical methods and ecological impacts, J Chem Technol Biotechnol, 37, 1045, https://doi.org/10.1002/jctb.6334, 2020.

Zhang, G. S. and Liu, Y. F.: The distribution of microplastics in soil aggregate fractions in southwestern China, The Science of the Total Environment, 642, 12–20, https://doi.org/10.1016/j.scitotenv.2018.06.004, 2018.